CHAPTER IV

RESULTS AND DISCUSSION

In this research, zinc oxide nanostructures were synthesized by using combined electrospinning and solvothermal techniques. Effects of many factors involving in this synthesis were investigated and will be described in this chapter.

4.1 Properties of As-spun PVA/Zinc Acetate Composite Fibers

PVA/zinc acetate composite fibers were prepared by electrospining of the spinning solution that was composed of zinc acetate and poly(vinyl alcohol) (PVA; M_w of 72,000) as starting materials and water as solvent. This solution is referred to as the spinning solution. By applying electric field strength across the syringe needle and the collector plate, ultrafine fibers were spun and deposited as a non-woven mat on the collector plate. The effects of PVA/zinc acetate ratio on morphology of the composite fibers are shown in Figure 4.1. It should be noted that the applied electric field strength was fixed at 19 kV/15 cm and PVA concentration in the spinning solution was 8 wt.%. The obtained composite fibers have smooth surface with diameter in nanometer scale. Using present concentration of PVA, the average fiber diameter of pure PVA fibers is 144 nm. By adding zinc acetate into the electrospinning solution, the obtained electrospun fibers are bigger than the pure PVA fibers. As the concentration of zinc acetate is increased, i.e. PVA/zinc acetate ratio is decreased, not only that diameter of the composite fibers increases but the size distribution of the fibers becomes broader as well. The frequency distribution of the electrospun fiber diameter is presented in Figure 4.2. The fiber diameters were measured by an image processing program (SemAfore 4.0), which randomly selected about 80 fibers from SEM images. It can be clearly observed that fiber size distribution becomes gradually broader with decreasing PVA/zinc acetate ratio in the spinning solution. The average diameter of the PVA/zinc acetate composite fibers with PVA-to-zinc acetate ratio of 3.0, 1.5 and 1.0 is 174, 210 and 383 nm, respectively.

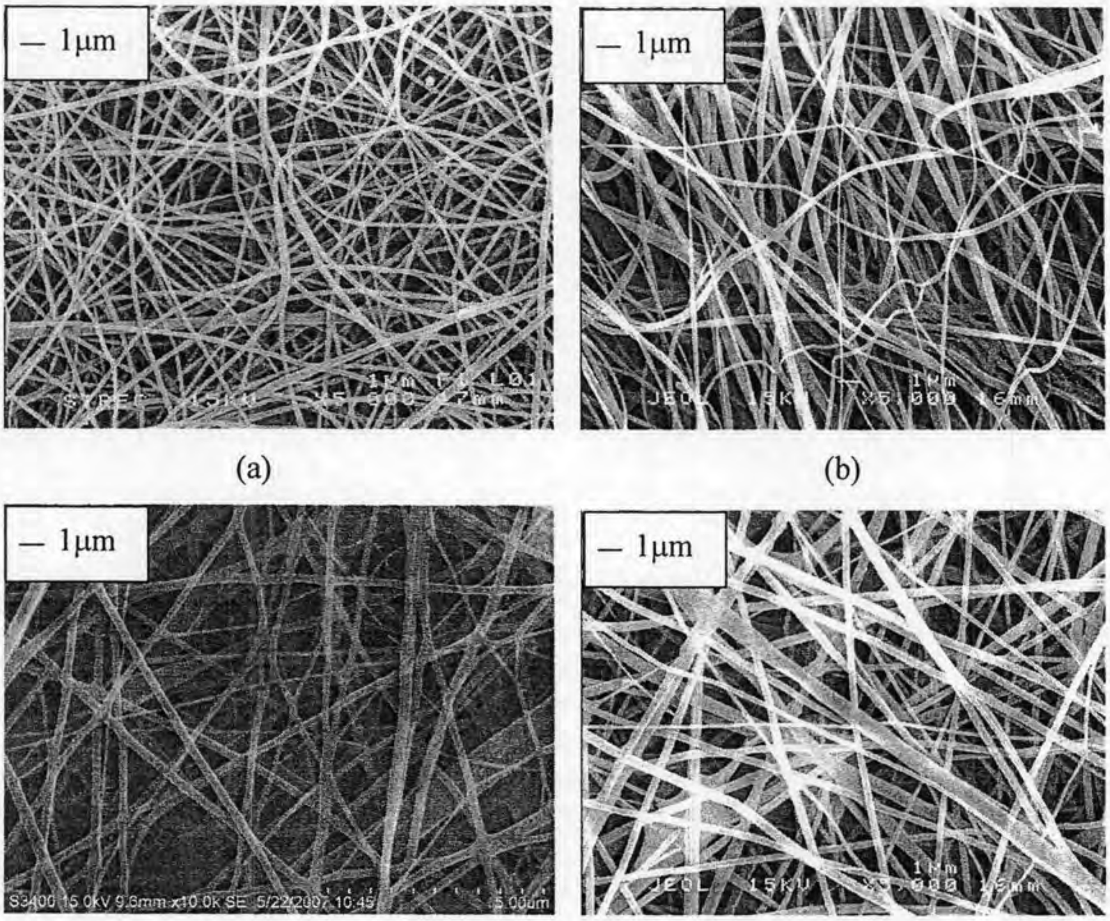

(a) (b)

(c) (d)

Figure 4.1 SEM images of the as-spun fibers prepared from the spinning solution containing only PVA (a), and PVA/zinc acetate with the PVA-to-zinc acetate ratio 3.0 (b), 1.5 (c) and 1.0 (d).

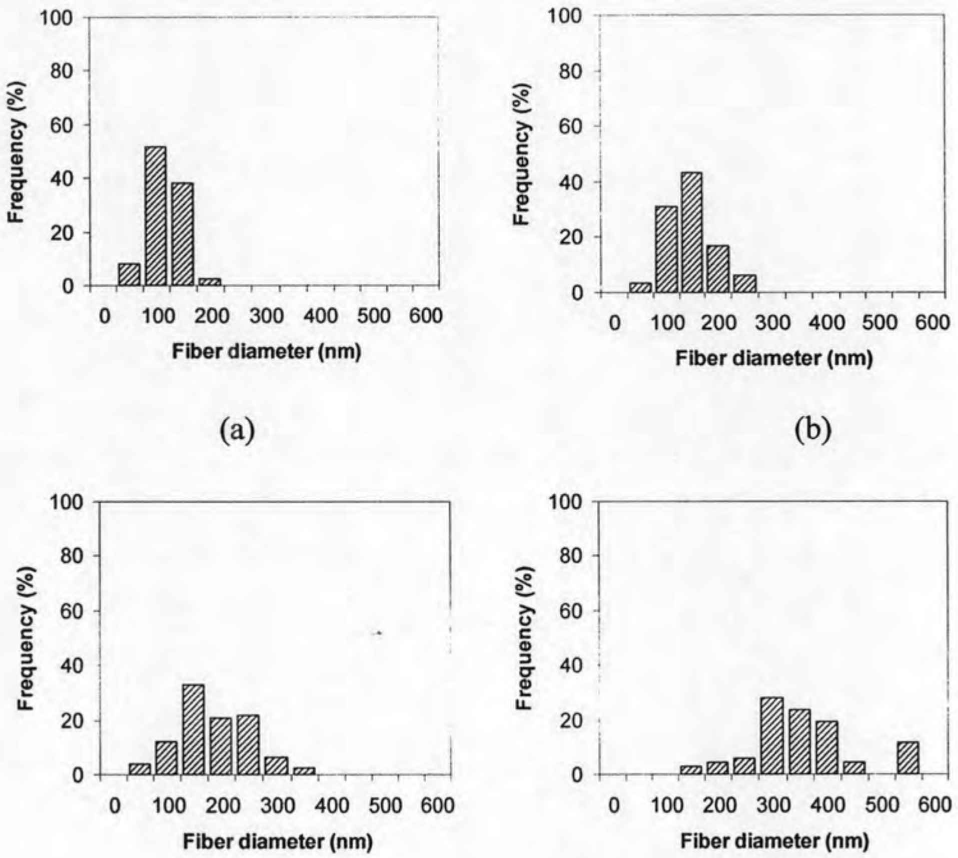

(a)

(b)

(c)

(d)

Figure 4.2 Frequency distributions of fiber diameter of the as-spun fibers prepared from the spinning solution containing only PVA (a), and PVA/zinc acetate with the PVA-to-zinc acetate ratio of 3.0 (b), 1.5 (c) and 1.0 (d).

Based on the results presented above, the concentration of zinc acetate has significant effect on the diameter of composite nanofibers. The increase in the average fiber diameter with increasing concentration of zinc acetate should be a result from the increase in viscosity of the spinning solution (Mit-uppatham et al., 2004). The increase in the viscosity of the spinning solution could also lead to non-uniform ejection of the jet, when the viscosity becomes too high (Frenot and Chronakis 2003; Huang et al., 2003). It is therefore responsible for broad size distribution of fibers prepared with high concentration of zinc acetate.

4.2 Conversion of the Composite Fibers into ZnO Nanostructure by Conventional Method

After the composite fibers were prepared, these fibers were left in air overnight. Then, these fibers were subjected to calcination at 600 °C for 2 hr to convert into ZnO fibers.

Thermal analysis of the as-spun fibers was conducted to determine the decomposition temperature of the precursor within the fibers. The result is shown in Figure 4.3. According to the TG result, most of the organic moieties from PVA, CH_3COO group of zinc acetate and other volatiles (e.g. H_2O, CO_x, etc.) are removed at temperature around 500 °C. As observed in the DTA curve, there are two endothermic peaks around 120 °C and 200 °C corresponding to the loss of absorbed water and decomposition of zinc acetate, which is in agreement with the weight loss of 30% in the TG curve. The exothermic peaks around 350 °C, 430 °C and 460 °C in the DTA curve may be the results from decomposition on the side and main chain of PVA (Yang et al., 2000). There is no further change in sample mass above 500 °C, indicating the formation of pure inorganic oxide.

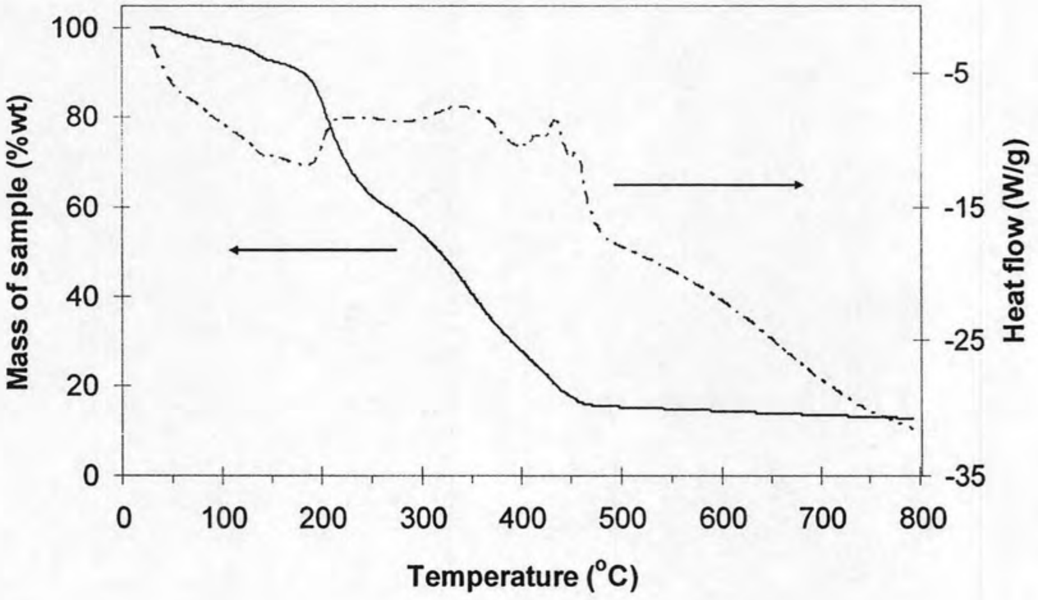

Figure 4.3 Thermogravimetric curves of the PVA/zinc acetate composite fibers analyzed in oxygen atmosphere using heating rate of 10 °C/min.

Figure 4.4 shows the FT-IR spectra for the as-spun composite fibers and the calcined ZnO fibers. The results indicate that all organic molecules could be removed completely from the fibers after calcination at 600 °C for 2 hr, since all the absorption bands associated with organic species (e.g., H_2O, CH, CO, OH, etc.) at wavenumber in the range of 800 – 1800 cm^{-1} are disappeared (Siddheswaran et al., 2006). Moreover, new band at around 553 cm^{-1}, which can be assigned to $\nu_{Zn\text{-}O}$ of ZnO (Hui et al., 2006), appears after calcination, indicating that the obtained fibers contain inorganic ZnO.

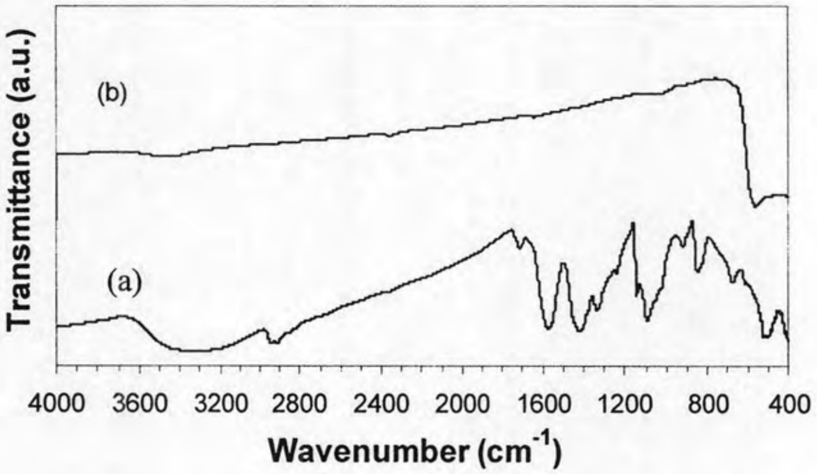

Figure 4.4 FT-IR spectra for: (a) PVA/zinc acetate composite fibers, (b) fibers calcined at 600 °C for 2 hr.

Figure 4.5 shows the XRD results for the as-spun composite fibers and the calcined fibers. As shown in Figure 4.5(a), the peak at around $2\theta = 20^{\circ}$ corresponds to (101) plane of semi-crystalline PVA in the composite fibers (Yang et al., 2000). This diffraction of PVA will be further confirmed with the XRD pattern of pure PVA in Section 4.3.3. Therefore, there might be interactions between PVA and zinc acetate molecules within the as-spun fibers. After the composite fibers were calcined at 600 °C for 2 hr, the peak corresponding to PVA disappears. All of the diffraction peaks observed are indexed to a wurtzite structure (hexagonal close packed) of ZnO as shown in Figure 4.5(b).

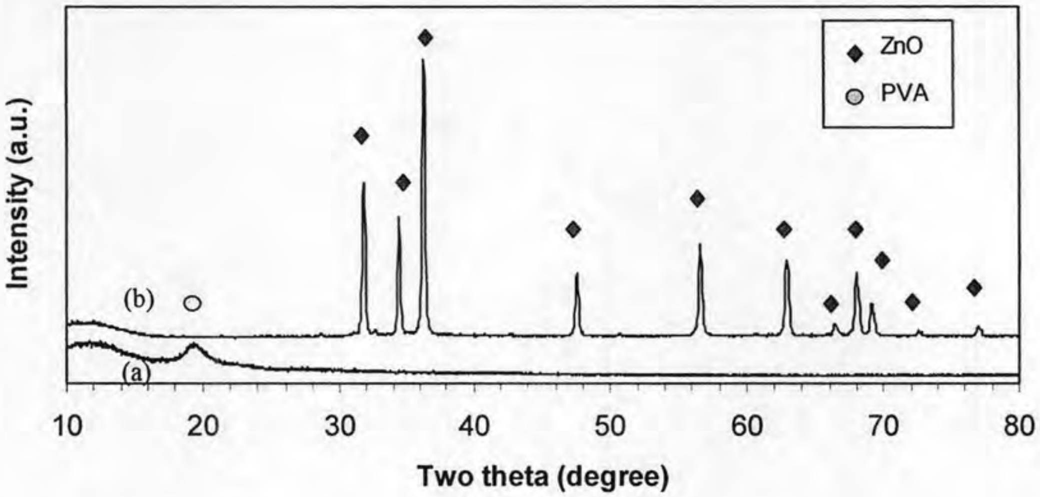

Figure 4.5 XRD results for: (a) PVA/zinc acetate composite fibers, (b) fibers calcined at 600 °C for 2 hr.

Morphology of the calcined fibers was observed by SEM. Figure 4.6 shows SEM image of the composite fibers with PVA/zinc acetate ratio of 1.5, after calcinations. Comparing with Figure 4.1(c), it can be observed that the calcined fibers have relatively smooth surface and uniform diameter around 150 nm. However, the ZnO fibers obtained exhibit significant shrinkage as well as the reduction in fiber diameter due to the decomposition of PVA and the removal of organic content, which has already been proved by TGA analysis.

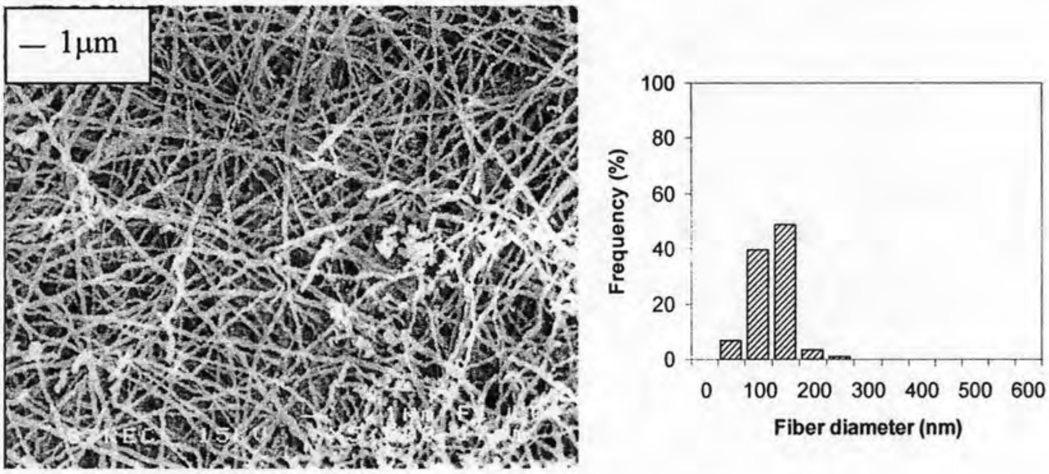

Figure 4.6 SEM image and size distribution of ZnO fibers calcined at 600 °C for 2 hr.

4.3 Conversion of the Composite Fibers into ZnO Nanostructure by Solvothermal Technique

4.3.1 *The Effect of PVA-to-Zinc Acetate Ratio*

Zinc oxide nanostructure was synthesized by the solvothermal reaction in 1-octanol at reaction temperature of 250 °C for 2 hr, using PVA/zinc acetate composite fibers as starting material. The ratio between PVA and zinc acetate in the fibers was varied from 3, 1.5 and 1. The XRD patterns of the ZnO nanostructures prepared, using various PVA-to-zinc acetate ratios are shown in Figure 4.7. All samples were ZnO in the hexagonal phase (wurtzite structure) without contamination from other crystalline phase. A similar intensity ratio of the diffraction peaks indicates that ZnO crystals grow along the same lattice direction.

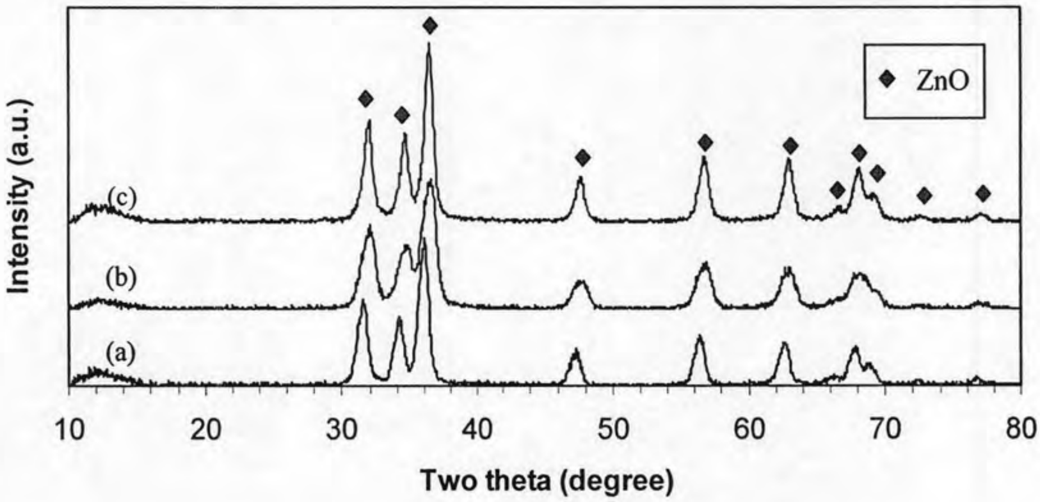

Figure 4.7 XRD results for ZnO nanostructures that were synthesized from PVA/zinc acetate composite fibers via the solvothermal reaction in 1-octanol at 250 °C for 2 hr, using PVA-to-zinc acetate ratio within the fibers of 3.0 (a), 1.5 (b) and 1.0 (c).

Figure 4.8 shows SEM images of ZnO nanostructures synthesized via the solvothermal technique in 1-octanol, using the composite fibers at various PVA/zinc acetate ratios as starting materials. It can be seen that ZnO nanostructures obtained are still in the fiber form, but the surfaces are rough. The fibers are consisting of small ZnO particles arranging into a form of fiber. In addition, some fibers are fused together and become larger structure.

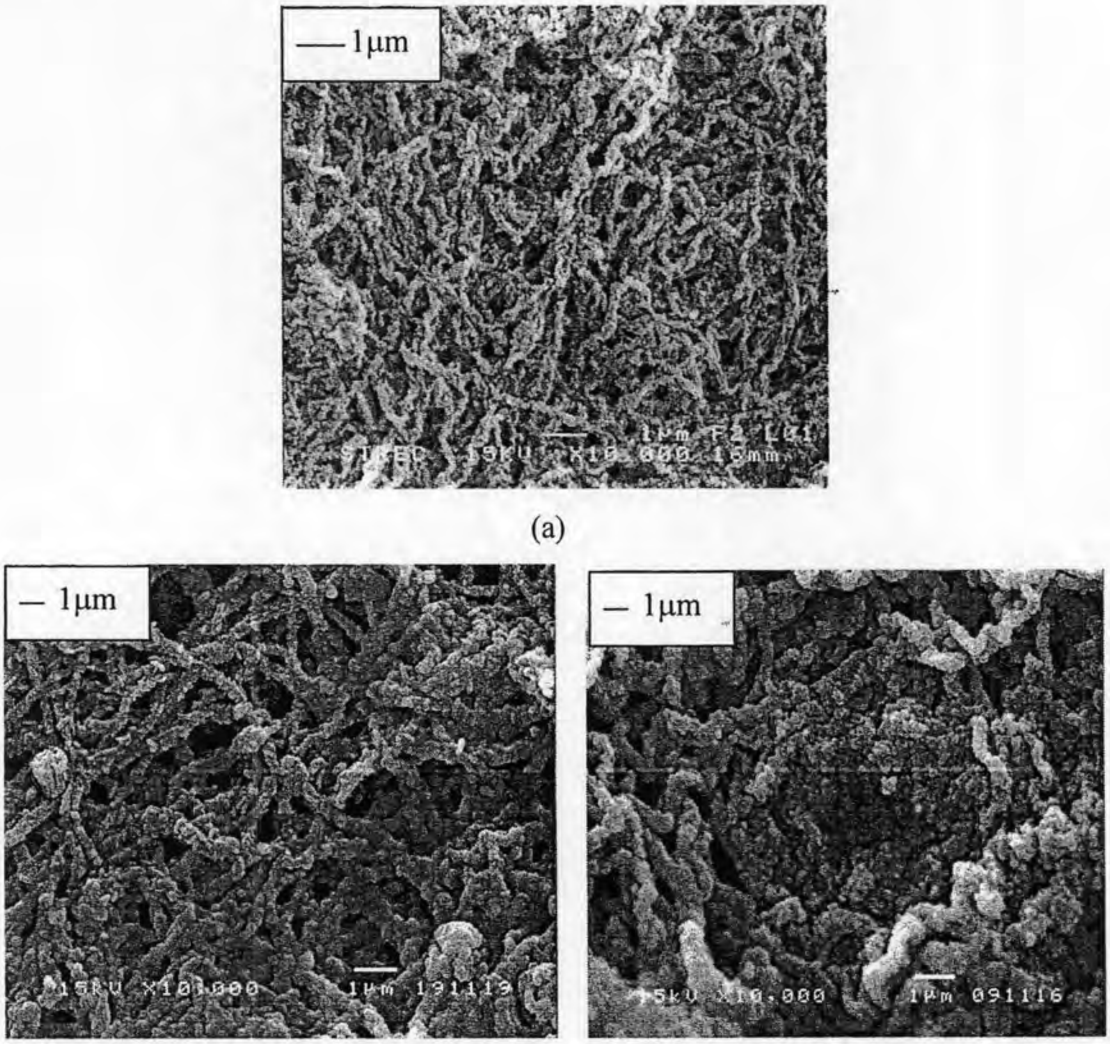

(a)

(b) (c)

Figure 4.8 SEM images of ZnO nanostructures that were synthesized from PVA/zinc acetate composite fibers via the solvothermal reaction in 1-octanol at 250 °C for 2 hr, using PVA-to-zinc acetate ratio within the fibers of 3.0 (a), 1.5 (b) and 1.0 (c).

As mentioned earlier, when the concentration of zinc acetate in the electrospinning solution is increased (i.e. low value of PVA-to-zinc acetate ratio), diameter of the as-spun composite fibers is increased. When the composite fibers were used as starting material in solvothermal process, the diameter of the final products (i.e. ZnO nanostructure) is also increased with the decreasing PVA-to-zinc acetate ratio.

The size distributions of the final products based on these SEM images are depicted Figure 4.9, analyzed using 80 fibers per sample. It is found that the size distribution of fibers becomes gradually broader with decreasing PVA-to-zinc acetate ratio because the frequency distribution of the composite fibers, which were used as starting materials, is also broader with decreasing PVA-to-zinc acetate ratio as described earlier in Section 4.1.

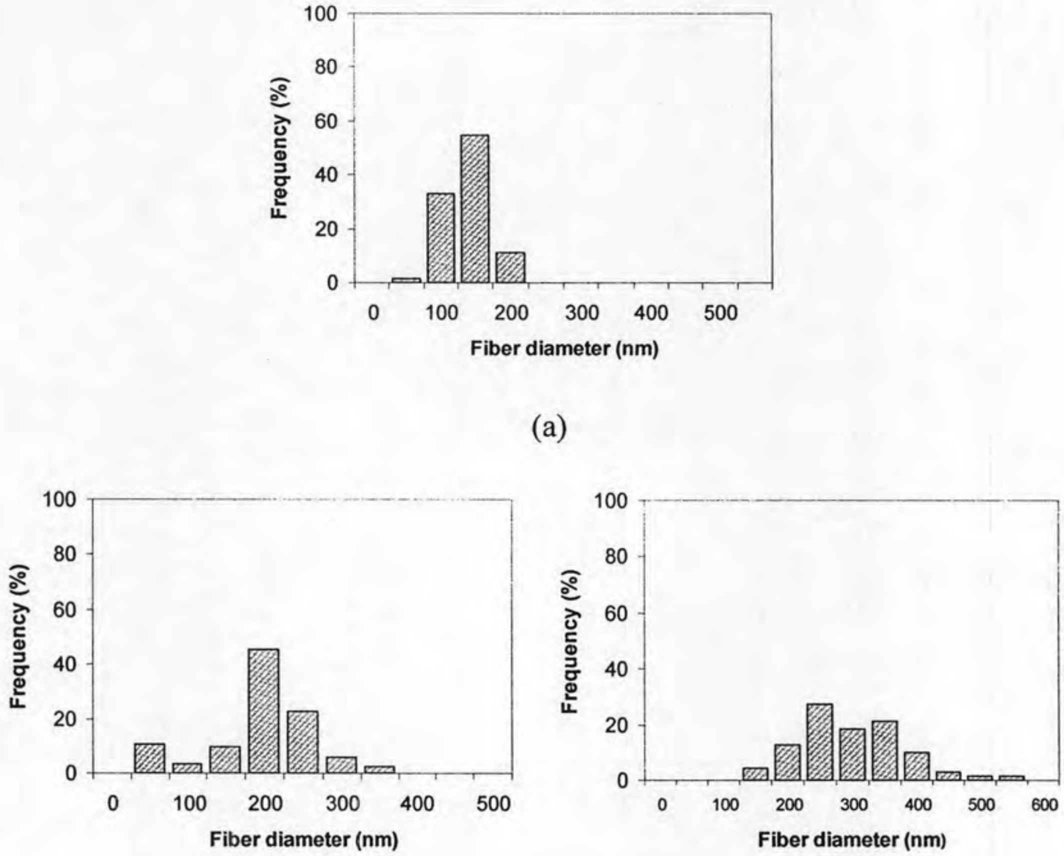

(a)

(b)

(c)

Figure 4.9 Frequency distribution for fiber diameters of the ZnO nanostructures that were synthesized from PVA/zinc acetate composite fibers via the solvothermal reaction in 1-octanol at 250 °C for 2 hr, using PVA-to-zinc acetate ratio within the fibers of 3.0 (a), 1.5 (b) and 1.0 (c).

Table 4.1 summarizes average fiber diameters of the as-spun PVA/zinc acetate composite fibers and the final products from the solvothermal process for various values of PVA-to-zinc acetate ratio. It can be seen that the fiber diameter of both the composite fibers and the final products are relatively similar. In some cases, the diameter of the final products is smaller than that of the composite fibers. The reduction in the size of fibers might be caused by the decomposition of some functional groups in PVA. In the other case, the fiber diameter of the final products is larger than that of the composite fibers. This is the result from fibers fusing together, yet the functional groups of PVA are also decomposed. Table 4.1 also shows crystallite sizes of the final products, calculated from the broadening of XRD pattern. It can be seen that, when PVA-to-zinc acetate ratio is decreased, (i.e. the concentration of zinc acetate is increased), the crystallite size of the final product is increased. This observation suggests that the increase in crystal growth with the number of nuclei sites (Tonto et al., 2006)

Table 4.1 Diameter of fibers and crystallite size of the ZnO nanostructures synthesize via the solvothermal technique, using PVA/zinc acetate composite fibers with various PVA-to-zinc acetate ratios as the starting material.

PVA-to-zinc acetate Ratio	*Average diameter of the as-spun composite fibers (nm)*	*ZnO nanostructures via solvothermal technique*	
		Average fiber diameter (nm)	*Crystallite size (nm)*
3.0	174	161	6.60
1.5	210	238	9.82
1.0	383	323	11.52

From visual observation of the final products, it can be seen that the final products still have elastic property of PVA. Figure 4.10 shows the FT-IR spectra for the composite fibers and the final products. As one can see that all the final products still have the functional groups of PVA polymer (broad absorption bands from 2,800 to 3,000 cm^{-1} and 800 to 1,800 cm^{-1}), although part of the organic moieties of PVA are removed from the composite fibers. The new absorption band around 533 cm^{-1} which is assigned to $\nu_{Zn\text{-}O}$ of ZnO (Hui et al., 2006), appears in all samples after the solvothermal process, confirming the XRD results that the products obtained contain inorganic ZnO.

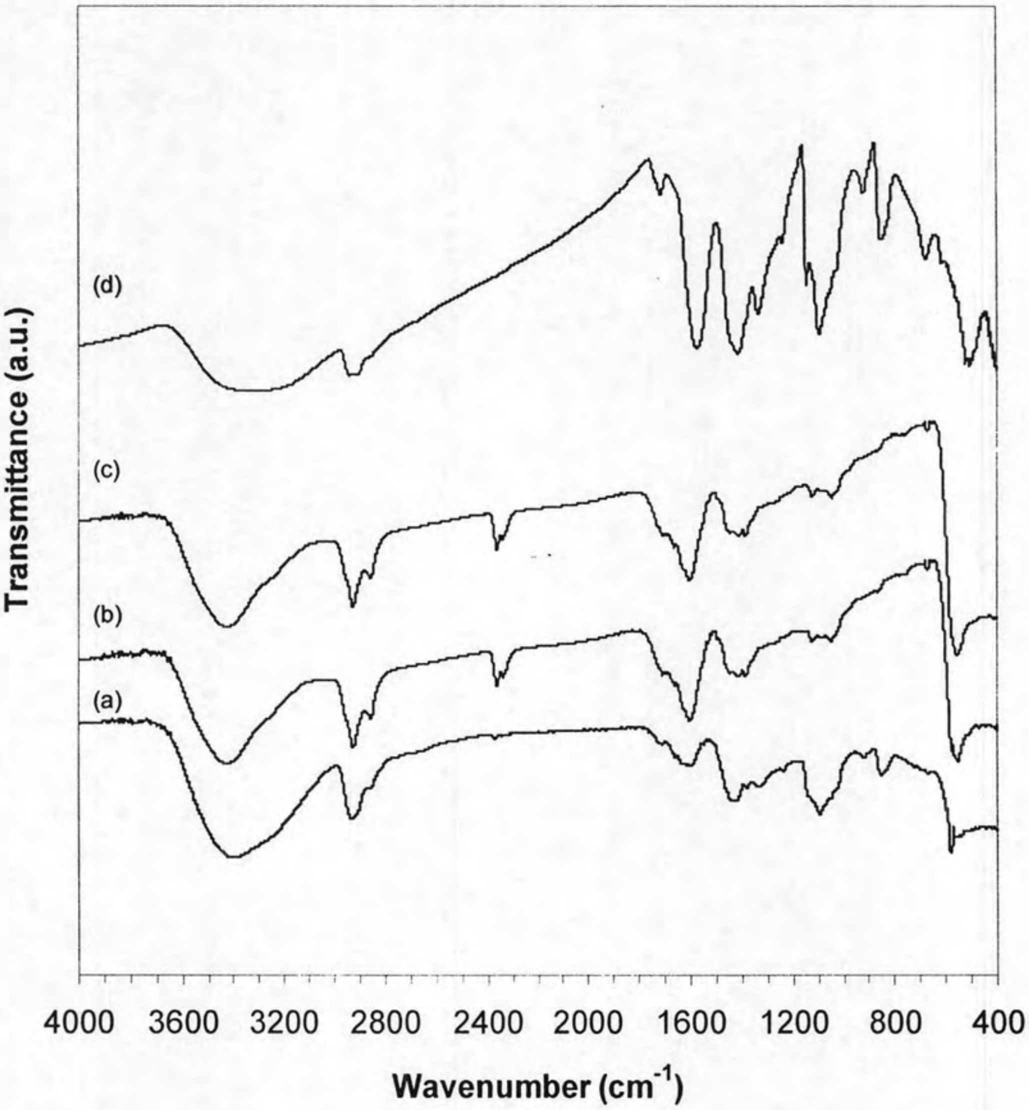

Figure 4.10 FT-IR spectra for ZnO nanostructures that were synthesized from PVA/zinc acetate composite fibers via the solvothermal reaction in 1-octanol at 250 °C for 2 hr, using PVA-to-zinc acetate ratio within the fibers of 3.0 (a), 1.5 (b), and 1.0 (c), comparing with that of PVA/zinc acetate composite fibers (d).

Figure 4.11 compares the TG curves of ZnO nanostructures synthesized via the solvothermal technique at 250 °C for 2 hr and that of pure PVA fibers. It is found that, for the ZnO nanostructures, mass loss about 20% takes place at temperature up to 500 °C, beyond which there is no change in sample mass. This behavior is similar to that of pure PVA, although the mass loss of pure PVA occurs in much greater extent. These results suggest that zinc acetate within the composite fibers can be converted into ZnO, while PVA is still retained.

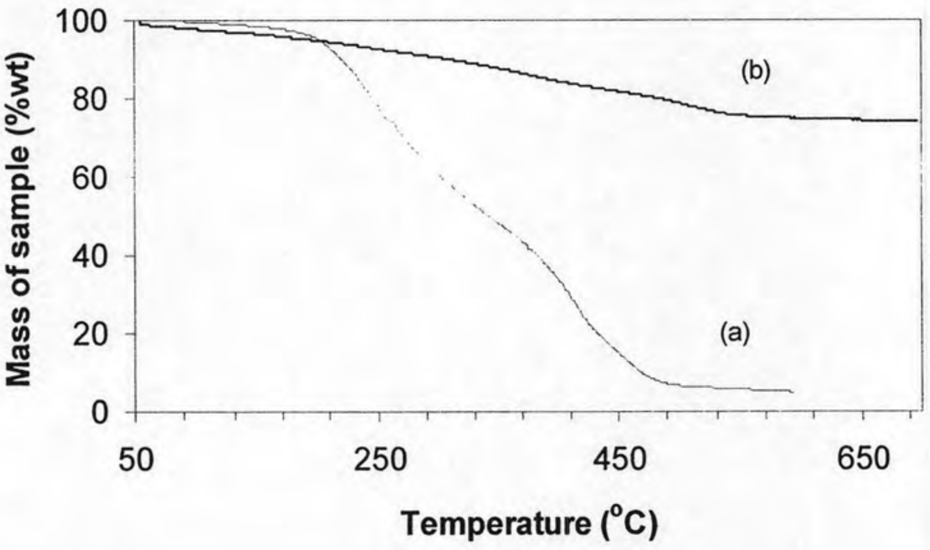

Figure 4.11 Thermogravimetric curves of pure PVA fiber (a) and ZnO nanostructure synthesized via solvothermal technique (b). The analyses were conducted in oxygen atmosphere.

4.3.2 *The Effect of Excess Zinc Acetate*

PVA/zinc acetate composite fibers and the excess zinc acetate powder were used as starting material in the solvothermal process. The amount of excess zinc acetate powder used was in the range of 0.1 – 10 g. The reaction was conducted at temperature of 250 °C for 2 hr.

The obtained products were separated into two parts, i.e. fibers part, which was the part of the product that possessed the shape of the composite fibers sheet originally placed into the system, and particles part, which was the powder formed in the reaction media outside the sheet of the composite fibers. Figure 4.12 and 4.13 shows the XRD results for the obtained products in fibers part and particles part, respectively. All samples were ZnO in the hexagonal phase (wurtzite structure) without contamination from other crystalline phase. A similar intensity ratio of the diffraction peaks indicates that ZnO crystals grow along the same lattice direction. The shift in XRD peaks of the fibers part (Figure 4.12) may be the result from the fact that shape of the bulk samples is not smooth and the samples could not be crushed into the powder form before testing by XRD, since the fibers part still contains PVA. The XRD peaks of the fibers part are wider than peaks for the particles part, which indicates that the crystallite size of the fibers part is smaller than the crystallite size for the particles part. This observation suggests that the polymer, i.e. PVA, inhibits the growth of ZnO nanocrystals within the fiber.

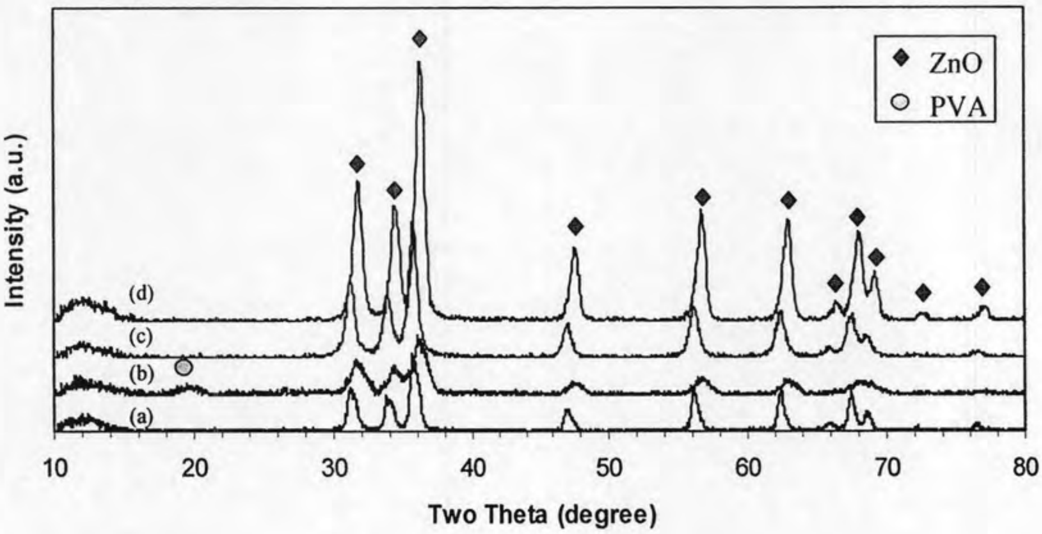

Figure 4.12 XRD results for fibers part in the ZnO nanostructures that were synthesized from PVA/zinc acetate composite fibers and the excess zinc acetate via the solvothermal reaction in 1-octanol at 250 °C for 2 hr, using PVA-to-zinc acetate ratio of 1.5 and the excess zinc acetate of 10 (a), 5 (b), 1 (c) and 0.1 g (d).

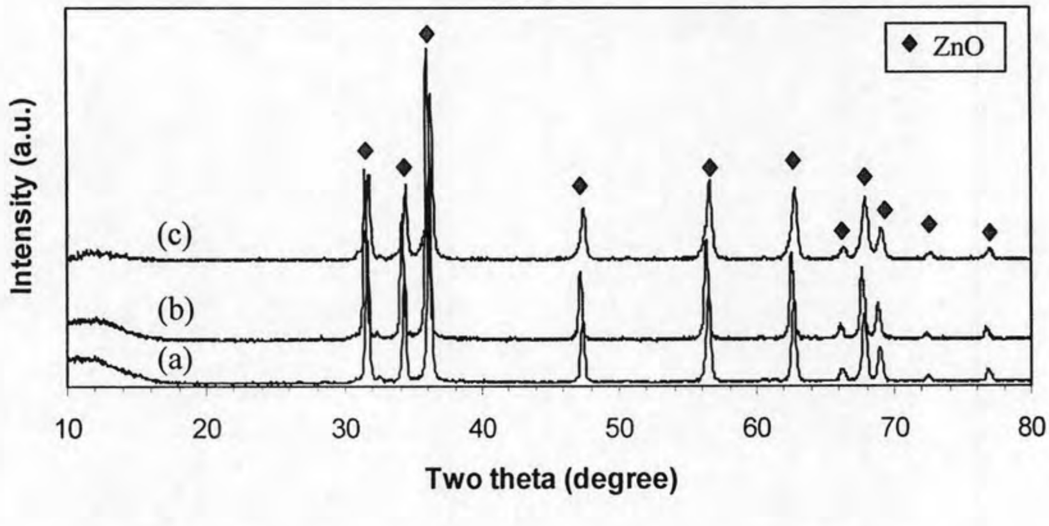

Figure 4.13 XRD results for particles part in the ZnO nanostructures that were synthesized from PVA/zinc acetate composite fibers and the excess zinc acetate via the solvothermal reaction in 1-octanol at 250 °C for 2 hr, using PVA-to-zinc acetate ratio of 1.5 and the excess zinc acetate of 10 (a), 5 (b) and 1 g (c).

During the synthesis of ZnO nanocrystals by wet chemical process (e.g. solvothermal process), zinc precursor is generally dissolved in the solution. During the reaction process, Zn^{2+} or its growth species can move freely in the solution to incorporate into nanocrystals. However, for the PVA/zinc acetate composite fibers, ZnO precursors are in a fixed state (i.e. these precursors are restricted inside solid PVA matrix). This means that the kinetics of nucleation and accretion as well as the formation mechanism for ZnO nanocrystals are completely different from the other wet chemical processes (Hong et al., 2006)

Figure 4.14 shows SEM image of the ZnO nanostructure that was synthesized in 1-octanol at 250 °C for 2 hr by using the composite fibers with PVA-to-zinc acetate ratio of 1.5 and additional 0.1 g of zinc acetate powder as starting materials. For this condition, only the fibers part was recovered after the reaction because the particles part was found in such small quantity that it was washed away and could not be collected. It was found that ZnO nanostructure obtained was still in the fiber form with average fiber diameter of 664 nm, measured by an image processing program (SemAfore 4.0). The fibers are consisting of particles arranging into a form of fiber. Size distributions of such particles are shown in Figure 4.15. It can be observed that these fibers are larger than the PVA/zinc acetate composite fibers used as the starting material because the fibers are attached by particles that are formed from the decomposition of the additional zinc acetate powder put into the same reaction system.

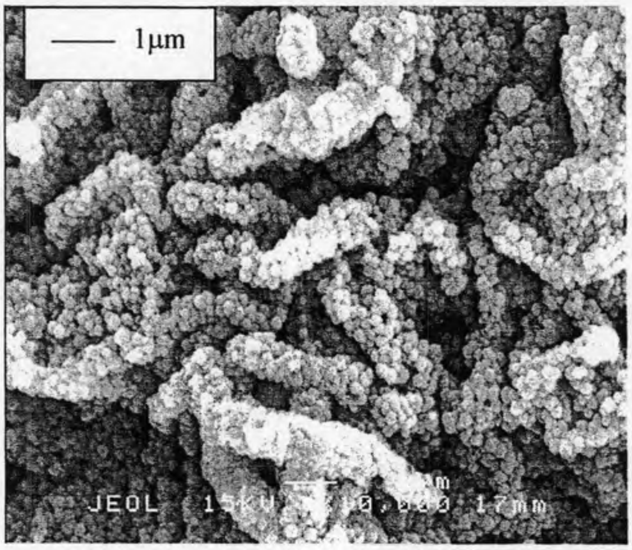

Figure 4.14 SEM image of ZnO nanostructures that were synthesized from PVA/zinc acetate composite fibers with PVA-to-zinc acetate ratio of 1.5 and the excess zinc acetate powder of 0.1 g via the solvothermal reaction in 1-octanol at 250 °C for 2 hr.

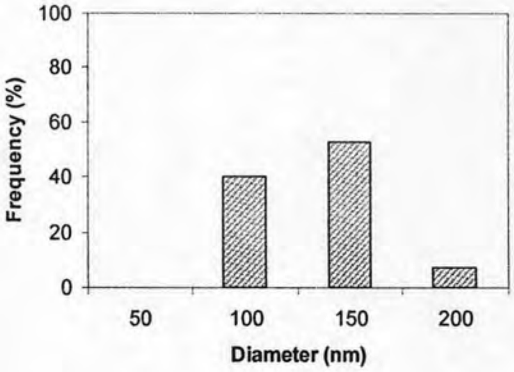

Figure 4.15 Frequency distribution for size of particles within the fibers of ZnO nanostructures that were synthesized from PVA/zinc acetate composite fibers with PVA-to-zinc acetate ratio of 1.5 and the excess zinc acetate powder of 0.1 g via the solvothermal reaction in 1-octanol at 250 °C for 2 hr.

Figure 4.16 shows SEM images of ZnO nanostructures that were synthesized by the same condition as above, but amount of the additional zinc acetate powder put into the system was increased to 1 g. For this synthesis condition, since amount of excess zinc acetate powder placed into the system was significant, the portion of the powders part was also substantial. The obtained products have the same morphological features as previously obtained products, but the fiber diameter as well as the diameter of particles forming into the fibers are larger than those of the previously obtained products. It can be seen that when the quantity of excess zinc acetate is increased, the fibers are more covered by particles formed from the decomposition of zinc acetate precursor additionally put into the system. Size distributions of particles within each part of the obtain nanostructures are shown in Figure 4.17. For the particles part shown in Figure 4.16(b), it can be observed that it is consisting of small particles with diameter 58 nm, which are smaller than the particles within the fibers. Thus, the particles within the fiber may not be pure ZnO as the small particles in the particles part, although the XRD results indicated they are consisting of ZnO. It is expected that certain amount of amorphous materials are residing in the particles forming in to the fibers.

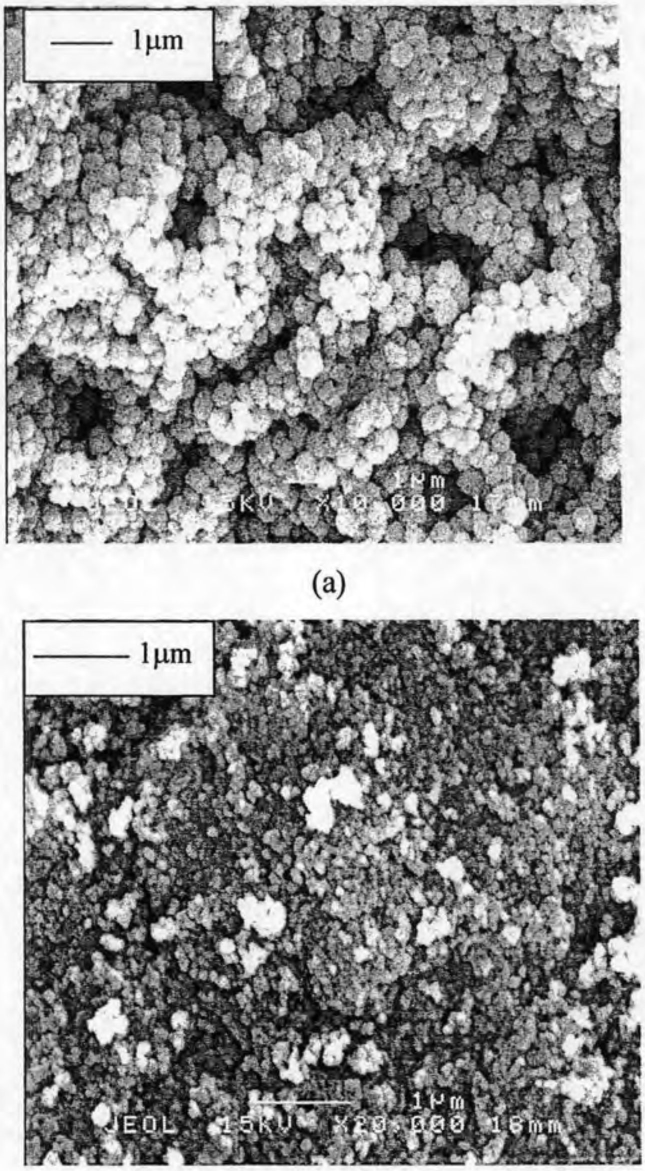

(a)

(b)

Figure 4.16 SEM images of ZnO nanostructures that were synthesized from PVA/zinc acetate composite fibers with PVA-to-zinc acetate ratio of 1.5 and the excess zinc acetate powder of 1 g via the solvothermal reaction in 1-octanol at 250 °C for 2 hr: (a) fibers part and (b) particles part.

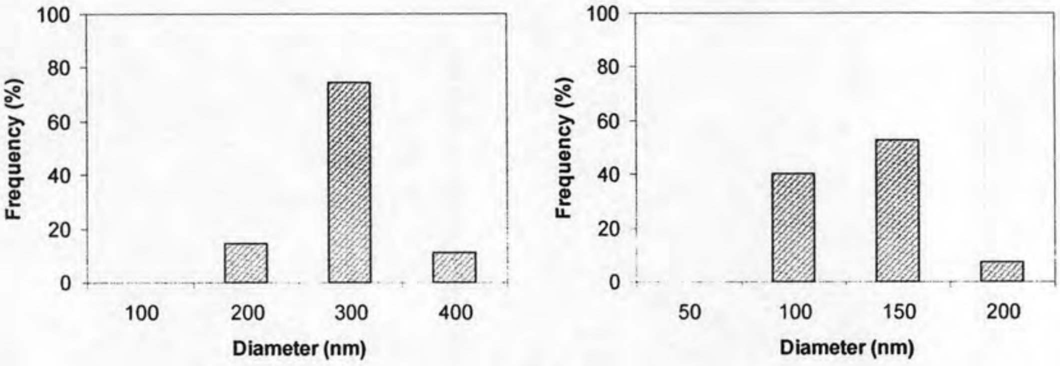

(a) (b)

Figure 4.17 Frequency distributions for size of particles within ZnO nanostructures that were synthesized from PVA/zinc acetate composite fibers with PVA-to-zinc acetate ratio of 1.5 and the excess zinc acetate powder of 1 g via the solvothermal reaction in 1-octanol at 250 °C for 2 hr: (a) fibers part and (b) particles part.

Figure 4.18 and Figure 4.19 show SEM images of ZnO nanostructures that were synthesized by increasing the amount of excess zinc acetate to 5 and 10 g, respectively. Figure 4.18(a) and 4.19(a) show the fibers part of obtained products, whereas it was found that the fiber form of the obtained product could no longer be seen because it was completely covered by the ZnO particles that were formed in large quantity from the excess zinc acetate. It is confirmed both average diameter and average length of the obtained products from the fibers part are similar to those obtained from the particles part.

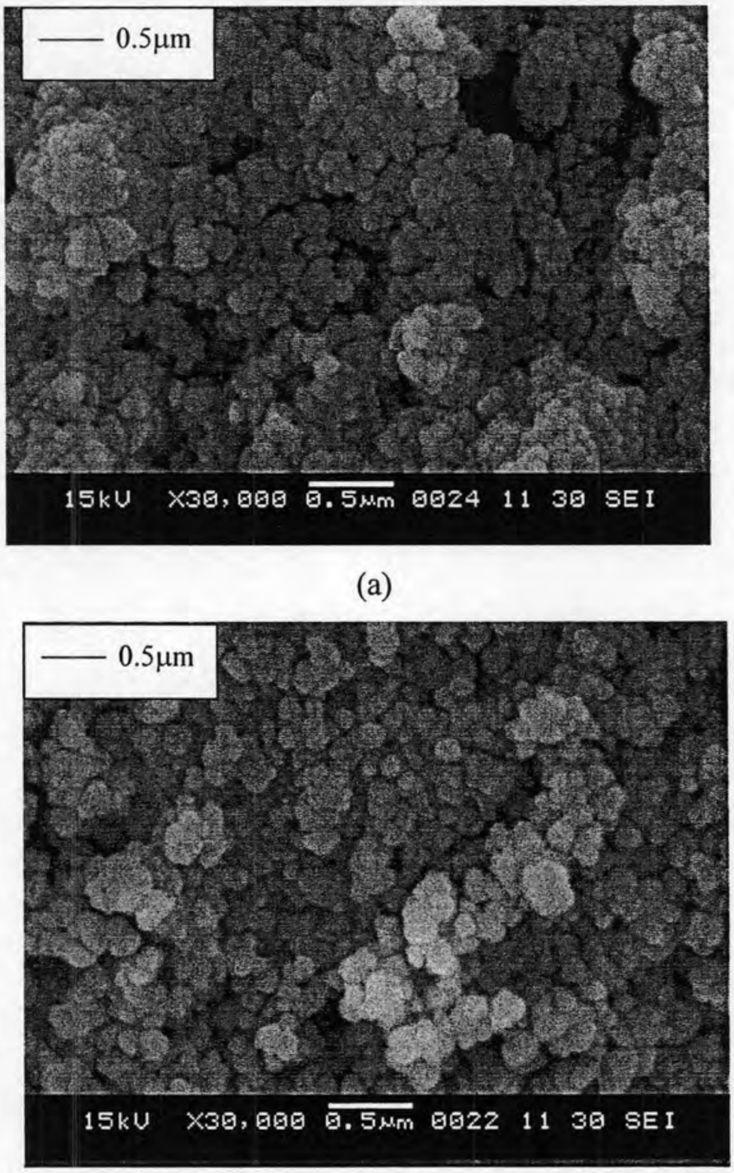

(a)

(b)

Figure 4.18 SEM images of ZnO nanostructures that were synthesized from PVA/zinc acetate composite fibers with PVA-to-zinc acetate ratio of 1.5 and the excess zinc acetate powder of 5 g via the solvothermal reaction in 1-octanol at 250 °C for 2 hr: (a) fibers part and (b) particles part.

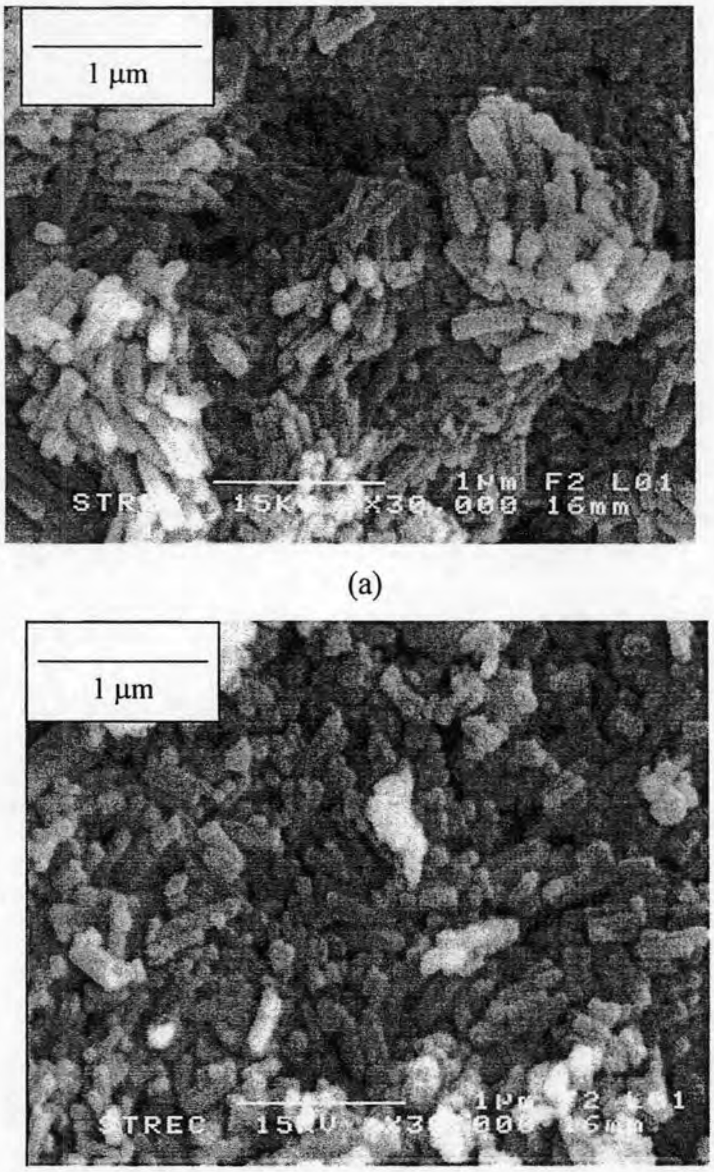

(a)

(b)

Figure 4.19 SEM images of ZnO nanostructures that were synthesized from PVA/zinc acetate composite fibers with PVA-to-zinc acetate ratio of 1.5 and the excess zinc acetate powder of 10 g via the solvothermal reaction in 1-octanol at 250 °C for 2 hr: (a) fibers part and (b) particles part.

Morphology of the obtained products from both conditions seemed to be nonporous nanorod with smooth surface. The diameter and length distributions based on these SEM images are depicted in Figure 4.20 and 4.21. Table 4.2 also summarizes dimension of ZnO nanostructures synthesized under various conditions. It is found that both average diameter and length of ZnO nanorods increased with an increase in the quantity of excess zinc acetate. This observation suggests the increase in crystal growth with the number of nuclei sites (Tonto et al., 2006).

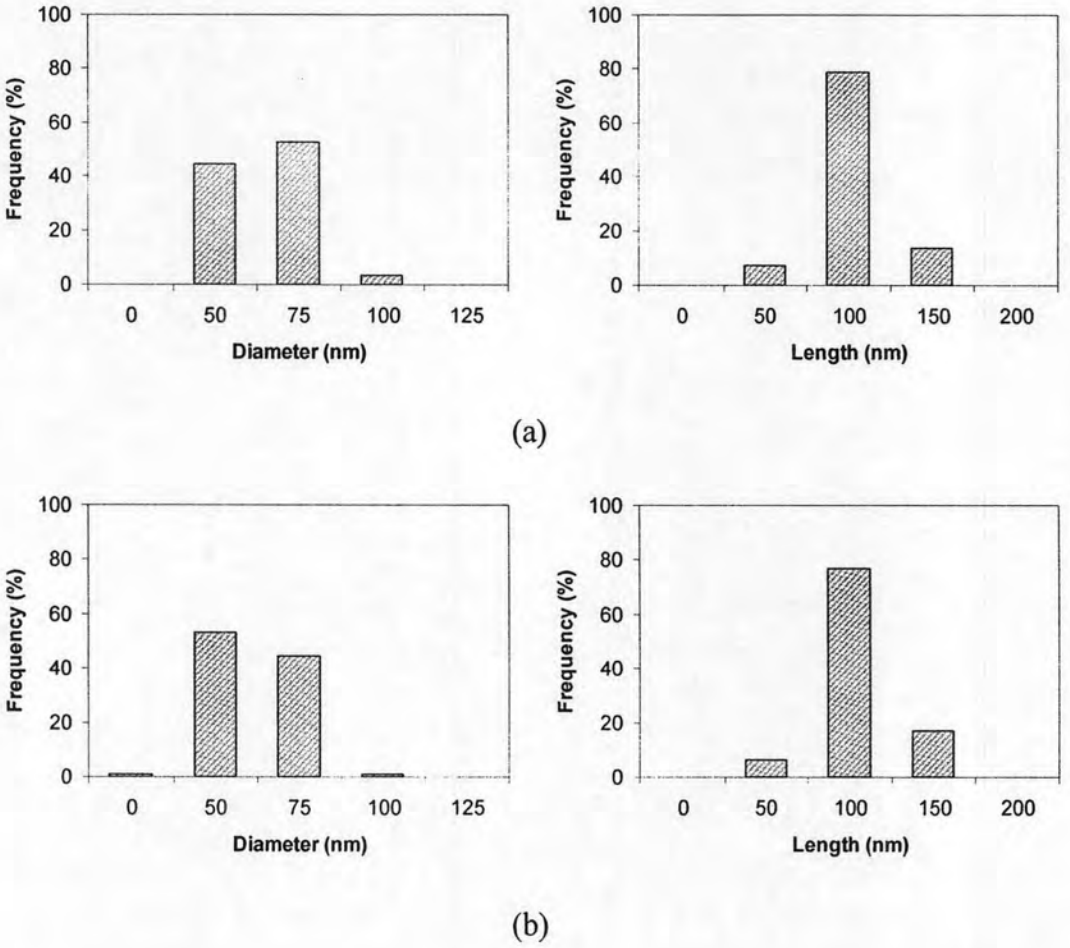

Figure 4.20 Frequency distributions for diameter and length of particles within ZnO nanostructures that were synthesized from PVA/zinc acetate composite fibers with PVA-to-zinc acetate ratio of 1.5 and the excess zinc acetate powder of 5 g via the solvothermal reaction in 1-octanol at 250 °C for 2 hr: (a) fibers part and (b) particles part.

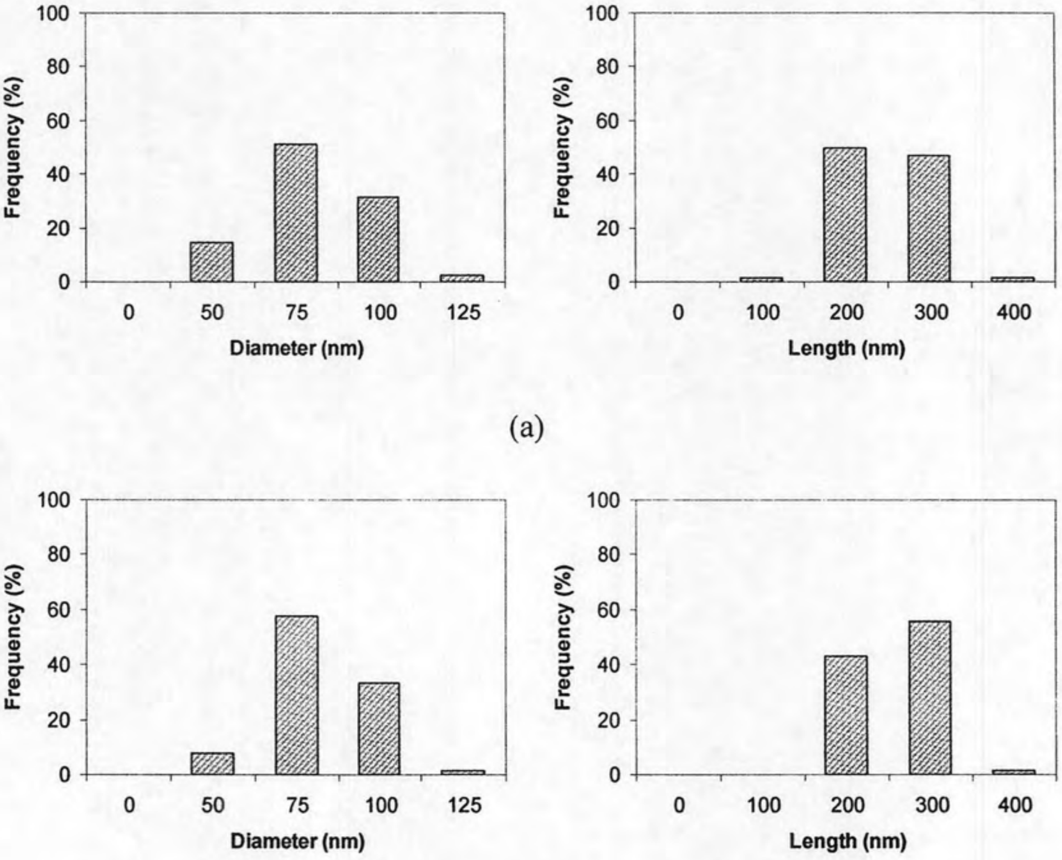

(b)

Figure 4.21 Frequency distributions for diameter and length of particles within ZnO nanostructures that were synthesized from PVA/zinc acetate composite fibers with PVA-to-zinc acetate ratio of 1.5 and the excess zinc acetate powder of 10 g via the solvothermal reaction in 1-octanol at 250 °C for 2 hr: (a) fibers part and (b) particles part.

Table 4.2 Dimension of ZnO nanostructure synthesized using various amounts of excess zinc acetate powder.

Amount of excess zinc acetate powder	*Part of ZnO nanostructure*	*Fiber diameter (nm)*	*Average diameter of particles forming into fibers (nm)*
0.1	*Fibers part*	664	157
	Particles part	-	-
1	*Fibers part*	1015	345
	Particles part	-	58
		Average diameter of particle (nm)	*Average length of particle (nm)*
5	*Fibers part*	77	128
	Particles part	74	131
10	*Fibers part*	95	299
	Particles part	95	302

The rate of crystal growth from any particular face was controlled by a combination of internal factors (e.g. intermolecular bonding preference or dislocation in crystal) and external factors (e.g. supersaturation condition, reaction temperature and type of solvent) (Kubota, 2001). For ZnO nanocrystals, the growth of the crystal is preferential in the *c*-axis forming into nanorods. However, it has been reported that the (0001) facet of the crystal, which is the slightly positively charged Zn surface, can adsorb negatively charged chemical species (Cheng and Samulski, 2004). In 1-octanol, which has low polarity because of the long chain length of the molecules, ZnO nanorods with high length can be obtained (Kunjara et al., 2006).

Figure 4.22 shows FT-IR spectra of the fibers part of the obtained products synthesized with various quantities of excess zinc acetate. It can be seen that all of the final products still have the functional groups of PVA polymer (broad peak from 2,800 to 3,000 cm^{-1} and 800 to 1800 cm^{-1}) (Hui et al., 2006), although part of the organic moieties of PVA are removed from the composite fibers.

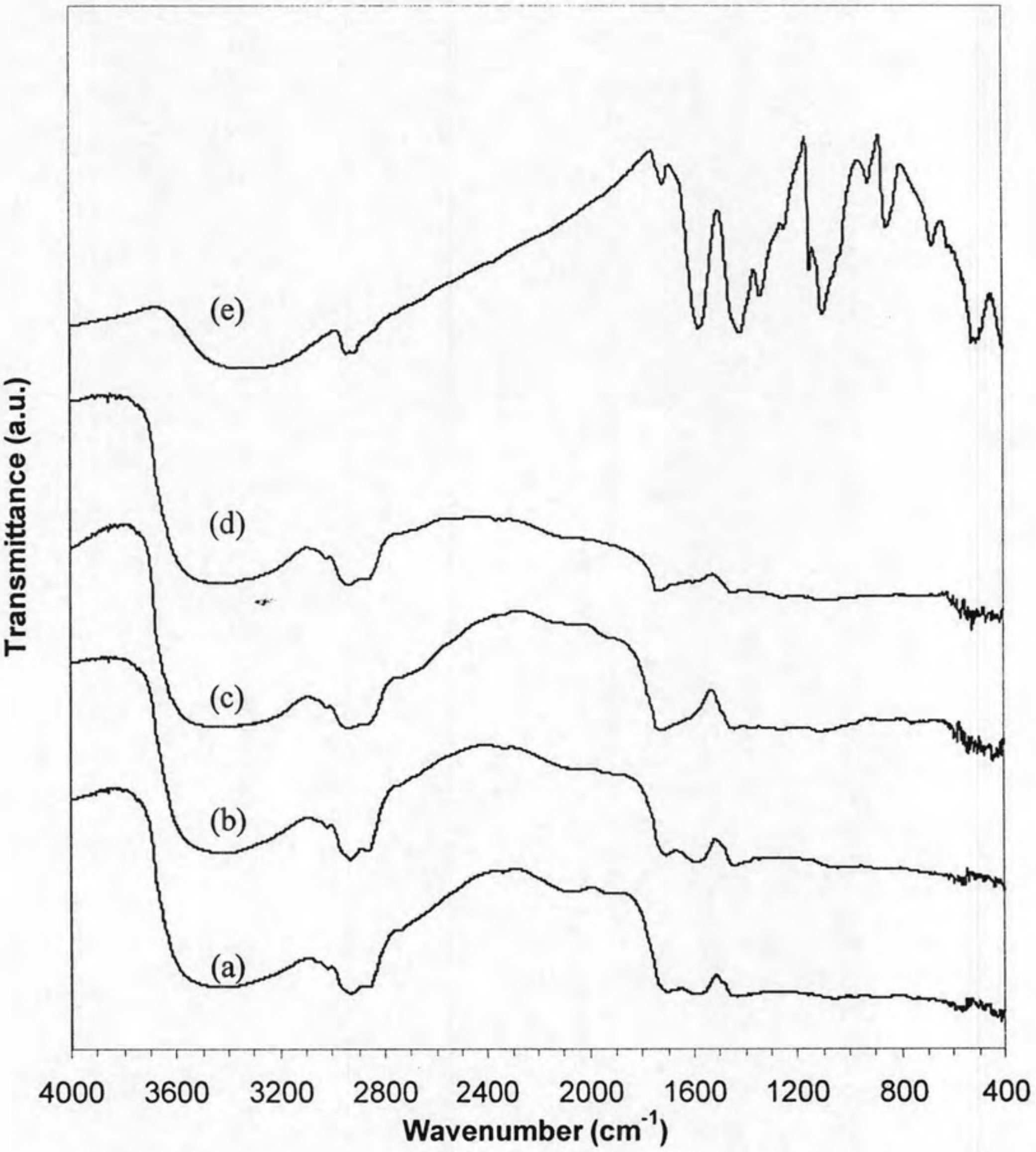

Figure 4.22 FT-IR spectra for the fibers part of ZnO nanostructures that were synthesized from PVA/zinc acetate composite fibers and the excess zinc acetate powder via the solvothermal reaction in 1-octanol at 250 °C for 2 hr, using PVA-to-zinc acetate ratio of 1.5 and the amount of excess zinc acetate of 0.1 (a), 1 (b), 5 (c) and 10 g (d), comparing with that of PVA/zinc acetate composite fibers (e).

Figure 4.23 shows the FT-IR spectra of the particles part of the obtained product synthesized with various quantities of excess zinc acetate. The obtained products have two broad peaks at about 1,451 and 1,600 cm^{-1}. With the increase in the quantity of excess zinc acetate, the intensity of these two bands are significantly decreased. These bands, which correspond to C=O stretching (1,585 cm^{-1}) and C–O stretching (1,444 cm^{-1}) vibration, are considered to be results from a variety of forms of acetate complex on the surface of ZnO particles (Sakohara et al., 1992, Sakohara et al., 1998, Shu et al., 2000). This observation suggests that zinc acetate was not completely converted into ZnO when amount of zinc acetate powder was too low because of the backward reaction between zinc acetate and 1-octanol that will be further discussed in Section 4.4. The ZnO species in the reaction may not be the solid ZnO because of low amount of excess zinc acetate. So, when amount of excess zinc acetate is decreased, the equilibrium may be shifted toward the reactant side, i.e. zinc acetate and 1-octanol.

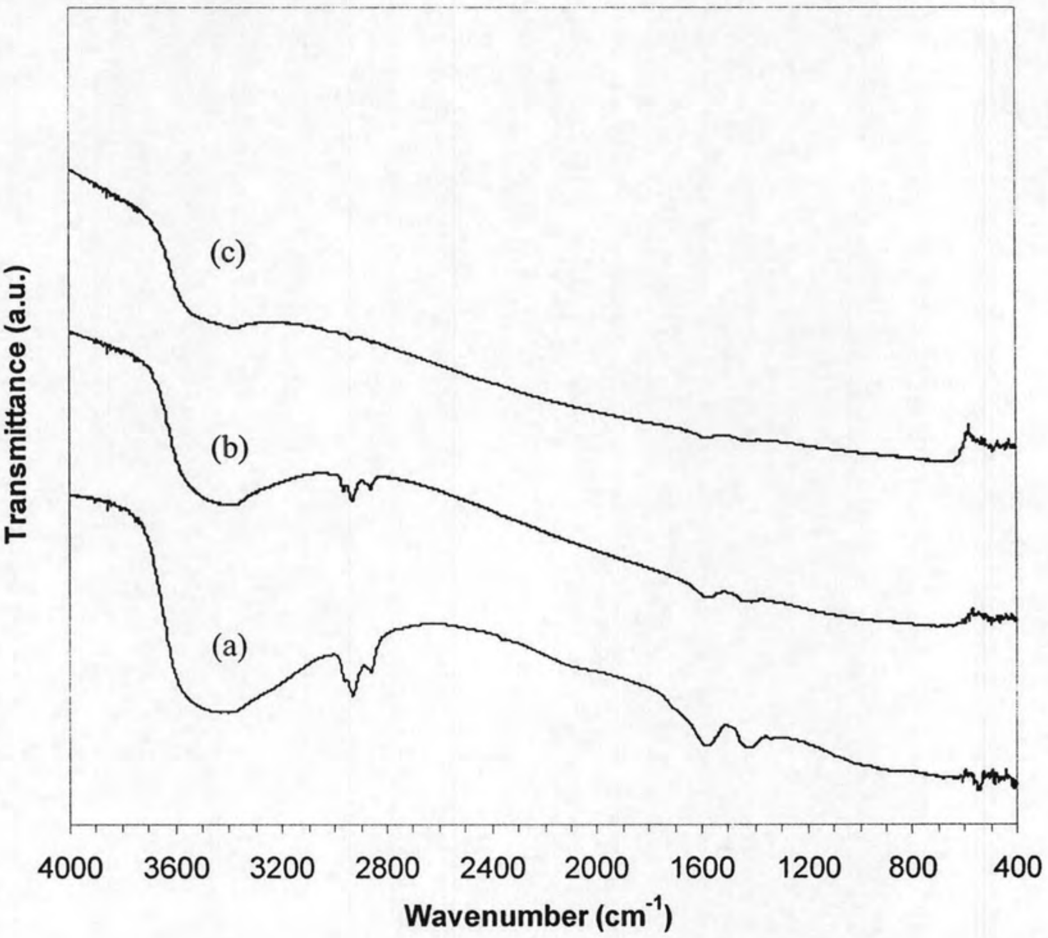

Figure 4.23 FT-IR spectra for the particles part of ZnO nanostructures that were synthesized from PVA/zinc acetate composite fibers and the excess zinc acetate powder via the solvothermal reaction in 1-octanol at 250 °C for 2 hr, using PVA-to-zinc acetate ratio of 1.5 and the amount of excess zinc acetate of 1 (a), 5 (b) and 10 g (c).

4.3.3 *The Effects of Reaction Temperature and Reaction Time*

ZnO nanostructure was synthesized by the solvothermal reaction in 1-octanol at various reaction temperatures and reaction times, using PVA/zinc acetate composite fibers and excess zinc acetate powder as starting materials. The discussions in this section is divided into two parts, i.e. when only PVA/zinc acetate composite fibers were used as starting material, and when both of PVA/zinc acetate composite fibers and the excess zinc acetate powder were used as starting materials for the solvothermal synthesis.

4.3.3.1 When only PVA/zinc acetate composite fibers were used as starting material

Figure 4.24 shows the XRD analysis results of the as-obtained products from the solvothermal process. All samples are ZnO in the hexagonal phase (wurtzite structure). A similar intensity ratio of the diffraction peaks indicates that ZnO crystals grow along the same lattice direction. Nevertheless, it is found that, for the ZnO nanostructures prepared under 200 °C for 2 hr, zinc acetate within the fibers is still not completely converted into ZnO (Figure 4.24d). The peaks at around 2θ of 22.5° and 41° corresponding to zinc acetate (Wu et al., 2007) are still observed. From visual observation of the obtained product, it can be seen that the product still has the elastic property of PVA polymer. This observation agrees with the fact that the peak at around $2\theta = 20^\circ$ corresponding to (101) plane of semi-crystalline PVA (Yang et al., 2000) is also found in the composite fibers. This peak disappears when the sample is synthesized at 250 °C. It indicates that the crystallinity of PVA is decreased when the reaction takes place at relatively high temperature. It should also be noted that the XRD peaks for zinc acetate disappears from the product synthesized at such high temperature as well.

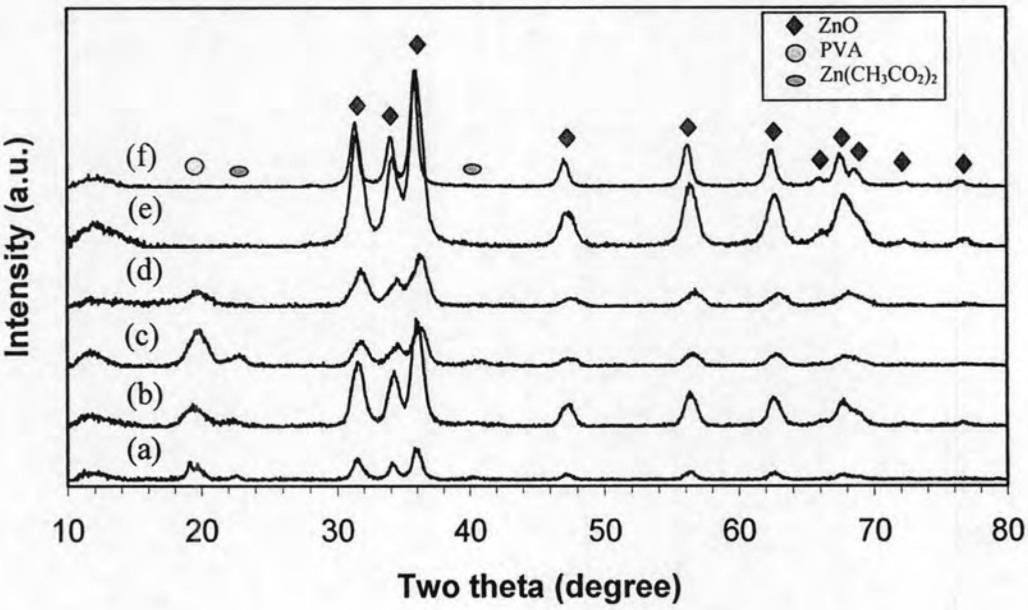

Figure 4.24 XRD results for ZnO nanostructures that were synthesized from PVA/zinc acetate composite fibers via the solvothermal reaction in 1-octanol at 170 °C for 0 hr (a), 170 °C for 2 hr (b), 200 °C for 0 hr (c), 200 °C for 2 hr (d), 250 °C for 0 hr (e) and 250 °C for 2 hr (f), using PVA-to-zinc acetate ratio of 1.5.

Figure 4.25 to 4.27 show SEM images of ZnO nanostructure synthesized at various reaction temperatures and reaction times. It can be seen that the obtained ZnO nanostructures are still in the fiber form although shape of the fiber is distorted. In addition, it seems like small particles are arranged to become fibers. Size distribution of fiber diameter and the diameter of particle within the fiber are shown in Appendix A1.

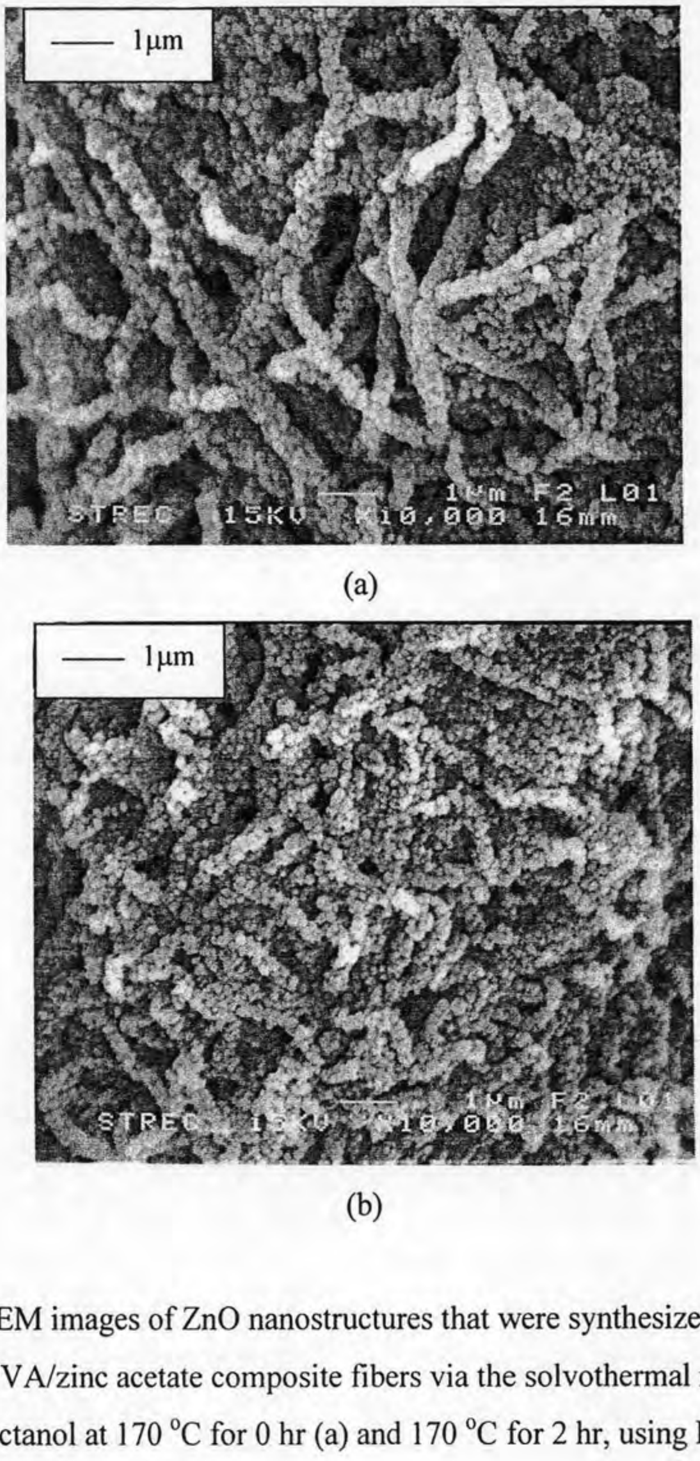

(a)

(b)

Figure 4.25 SEM images of ZnO nanostructures that were synthesized from PVA/zinc acetate composite fibers via the solvothermal reaction in 1-octanol at 170 °C for 0 hr (a) and 170 °C for 2 hr, using PVA-to-zinc acetate ratio of 1.5.

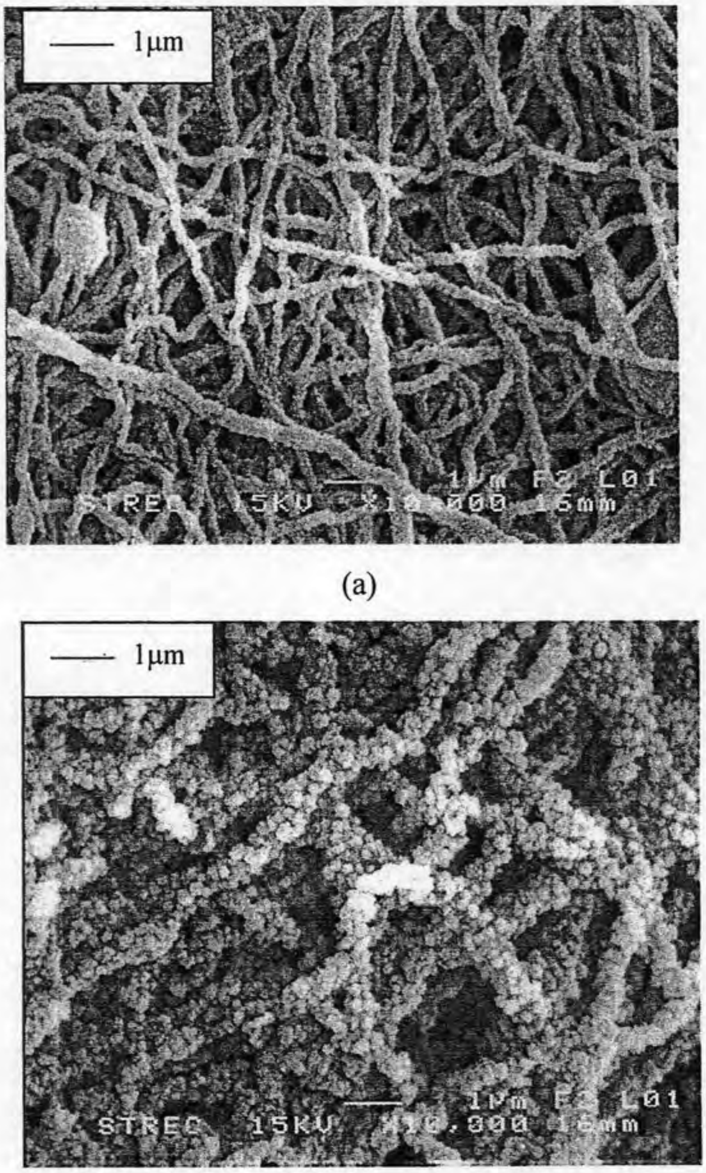

(a)

(b)

Figure 4.26 SEM images of ZnO nanostructures that were synthesized from PVA/zinc acetate composite fibers via the solvothermal reaction in 1-octanol at 200 °C for 0 hr (a) and 200 °C for 2 hr, using PVA-to-zinc acetate ratio of 1.5.

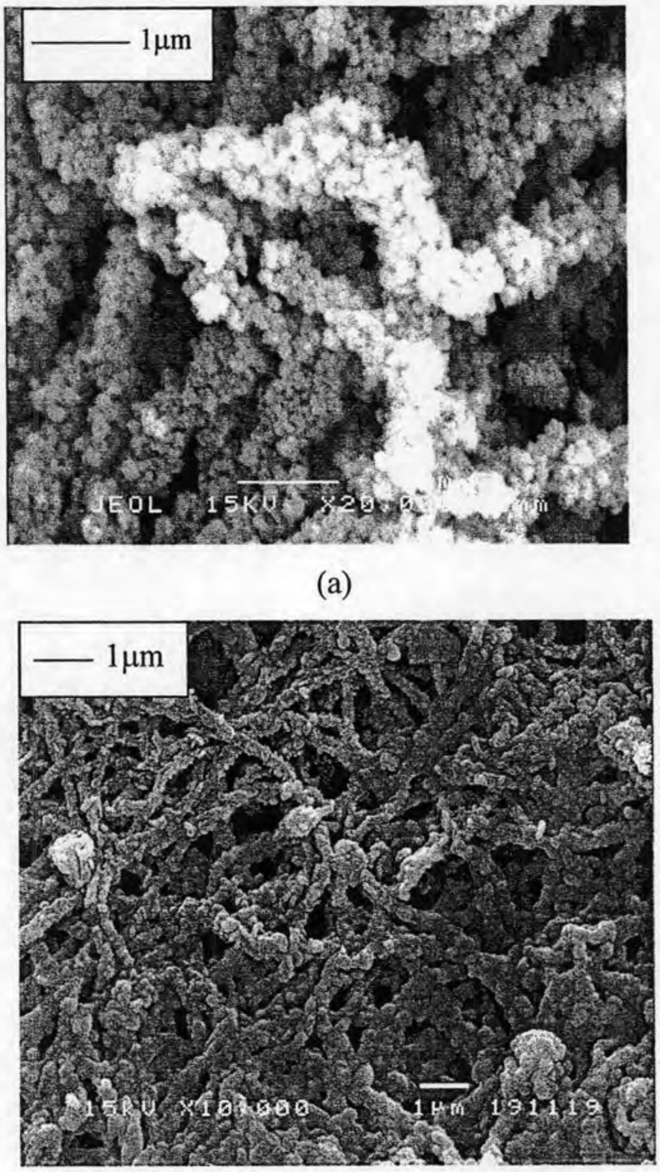

(a)

(b)

Figure 4.27 SEM images of ZnO nanostructures that were synthesized from PVA/zinc acetate composite fibers via the solvothermal reaction in 1-octanol at 250 °C for 0 hr (a) and 250 °C for 2 hr, using PVA-to-zinc acetate ratio of 1.5.

Figure 4.28 shows the average fiber diameter and average diameter of particles within the fiber measured from SEM images in Figure 4.25 to 4.27. It can be observed that, when the solvothermal process takes place at temperature below 200 °C, the average fiber diameter and average diameter of particles within the fiber show the similar trend with respect to the change in the synthesis conditions. At 170 °C, the average fiber diameter and average particle diameter increase when the reaction time is increased. This might relate to the fact that zinc acetate is not completely converted into ZnO and PVA still remains within the fiber as previously shown in the XRD results (Figure 4.24). PVA may be swollen or the partially decomposed zinc acetate within the fibers may aggregates into clusters as the solvothermal reaction proceeds. When the reaction temperature is increased to 200 °C, both diameters are smaller than the values of the products synthesized at 170 °C. It might be the result from the fact that zinc acetate starts to completely convert into ZnO at this temperature. However, if the reaction at 200 °C is held for 2 hr, the average size of particles within the fiber is increased because of the growth of ZnO crystallites. The growth of the ZnO crystals is more immense as the reaction temperature is raised to 250 °C. On the other hand, the average fiber diameter is decreased because PVA within the fibers is decomposed at this temperature.

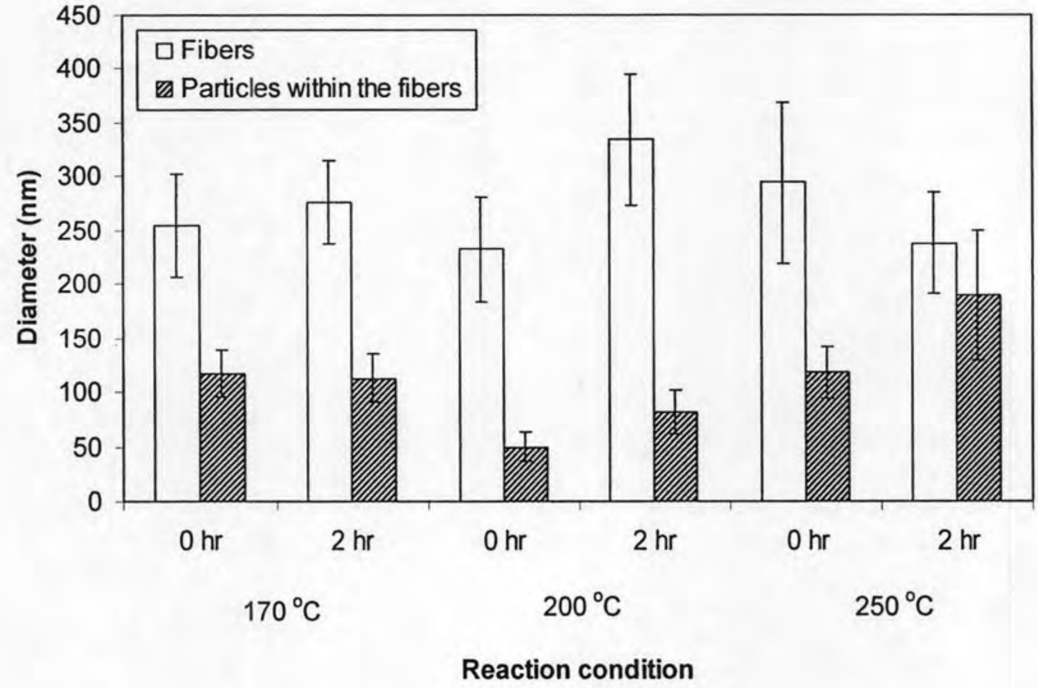

Figure 4.28 Average fiber diameter and average diameter of particles within the fibers of ZnO nanostructures that were synthesized from PVA/zinc acetate composite fibers via the solvothermal reaction in 1-octanol at various temperatures and reaction times, using PVA-to-zinc acetate ratio of 1.5.

Figure 4.29 shows the crystallite size of the ZnO nanostructure, calculated from the broadening of XRD pattern. It can be seen that the change in the crystallite size of the ZnO nanostructure according to the change in the reaction condition follows similar trend as that of average diameter of particles within the fibers. Nevertheless, it should be noted that the particle size is almost one order of magnitude larger than the crystallite size calculated. Therefore, all the particles embedded within the fibers are indeed polycrystalline. When the temperature is increased from 170 °C to 200 °C, the crystallite size is decreased. It might be the result from further the decomposition of remaining Zn-containing intermediates.

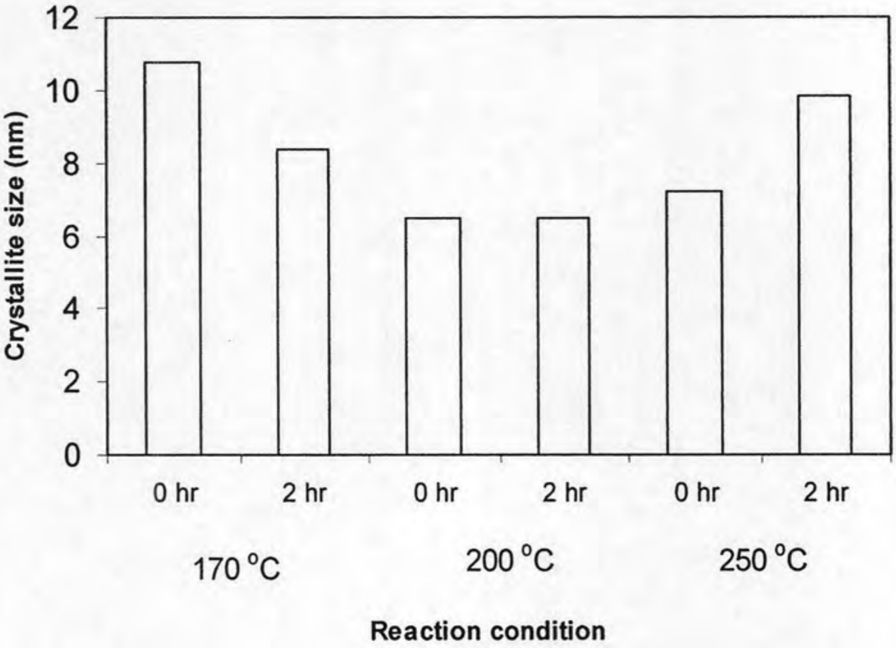

Figure 4.29 Crystallite size of ZnO nanostructures that were synthesized from PVA/zinc acetate composite fibers via the solvothermal reaction in 1-octanol at various temperatures and reaction times, using PVA-to-zinc acetate ratio of 1.5.

From visual observation of the obtained products, it can be seen that the obtained products still have elastic property of PVA. Figure 4.30 shows the FT-IR spectra for the composite fibers and the final products. It can be seen that all of the final products still have main functional groups of PVA polymer (broad absorption bands from 2,800 to 3,000 cm^{-1} and 800 to 1,800 cm^{-1}), although parts of the organic moieties of PVA are removed from the composite fibers. The new absorption band around 533 cm^{-1} which is assigned to $\nu_{\text{Zn-O}}$ of ZnO (Hui et al., 2006), appears in all samples after the solvothermal process, confirming the XRD results that the products obtained contain inorganic ZnO.

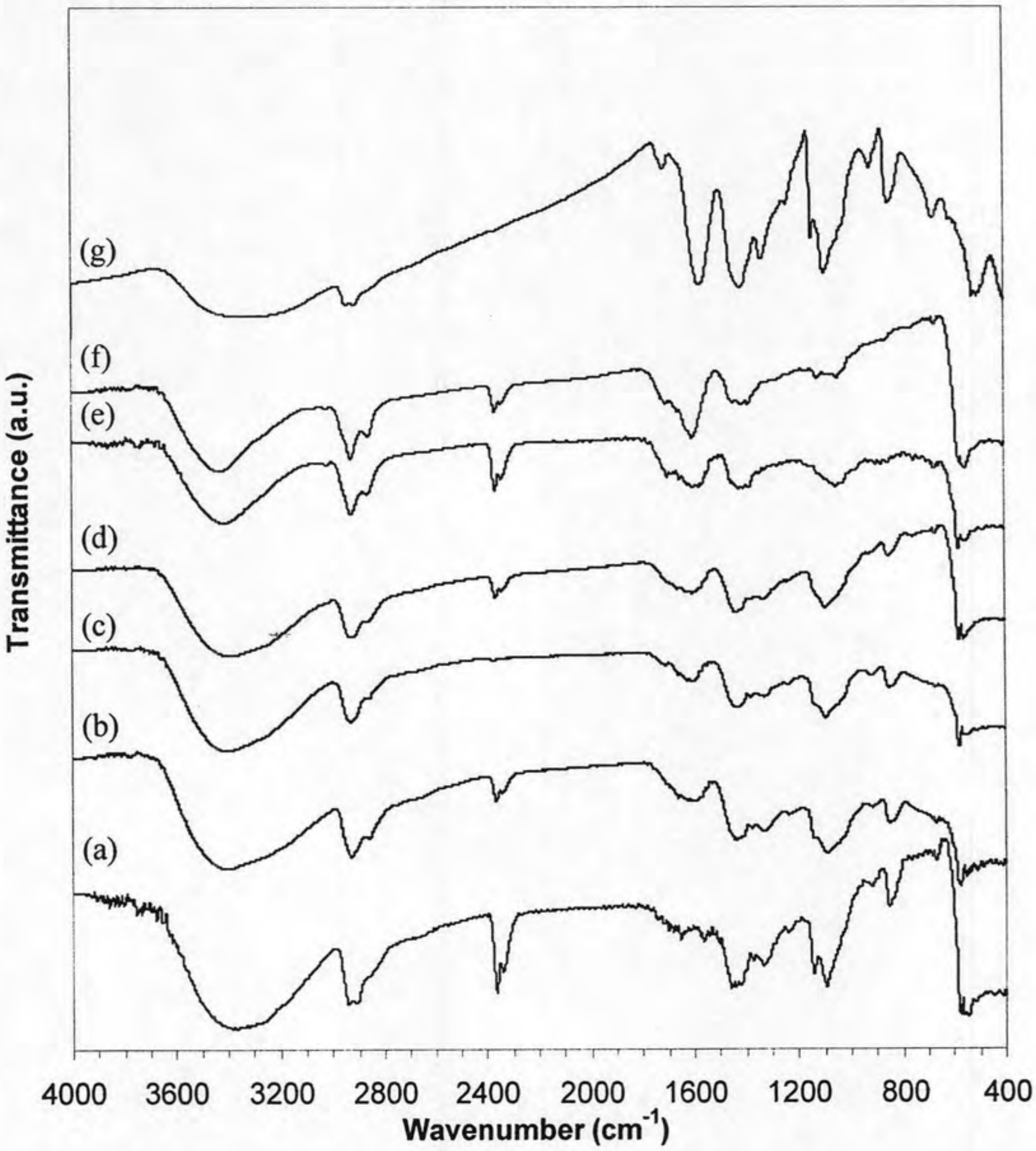

Figure 4.30 FT-IR spectra for ZnO nanostructures that were synthesized from PVA/zinc acetate composite fibers via the solvothermal reaction in 1-octanol at 170 °C for 0 hr (a), 170 °C for 2 hr (b), 200 °C for 0 hr (c), 200 °C for 2 hr (d), 250 °C for 0 hr (e) and 250 °C for 2 hr (f), comparing with that of PVA/zinc acetate composite fibers (g), using PVA-to-zinc acetate ratio of 1.5.

As a control for the experiment, pure PVA nanofibers were subjected to the same solvothermal process described earlier. Figure 4.31 shows the XRD results. It can be seen from a peak at around $2\theta = 20^{\circ}$ corresponding to (101) plane of semi-crystalline PVA (Yang et al., 2000) that this product still have the crystalline PVA. However the crystallinity of PVA in pure PVA sample is less than that of the original PVA before the reaction. From visual observation of the product, it can be seen that the products still have elastic property of PVA. Nevertheless, Figure 4.32 shows that the solvothermal product of the pure PVA fibers is no longer in fiber form because PVA dissolves in 1-octanol at this temperature. On the other hand, the PVA/zinc acetate fibers still remain in the fiber form. It is therefore suggested that zinc acetate within the fibers has converted into ZnO before PVA within the fibers is completely dissolved in 1-octanol.

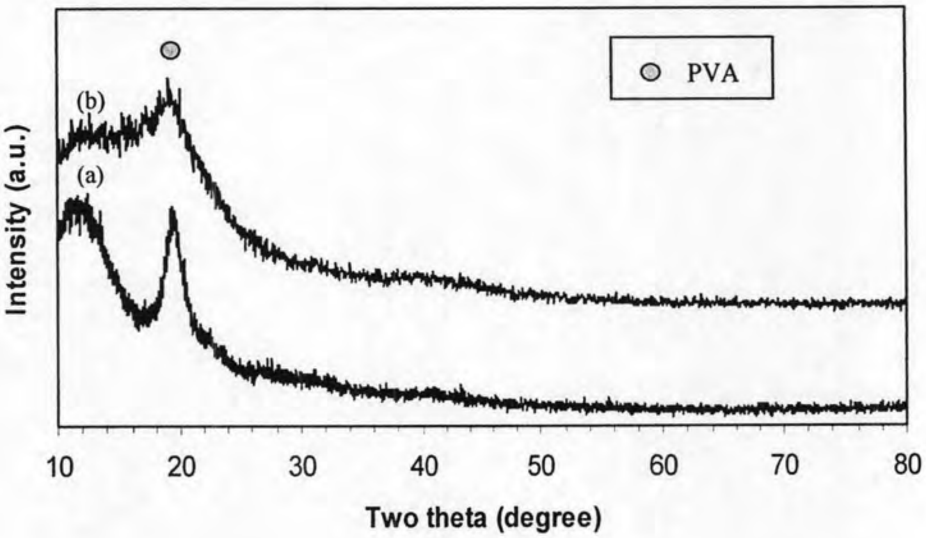

Figure 4.31 XRD results of pure PVA fibers (a) and PVA fibers after subjected to the solvothermal reaction in 1- octanol at 250 °C for 2 hr (b).

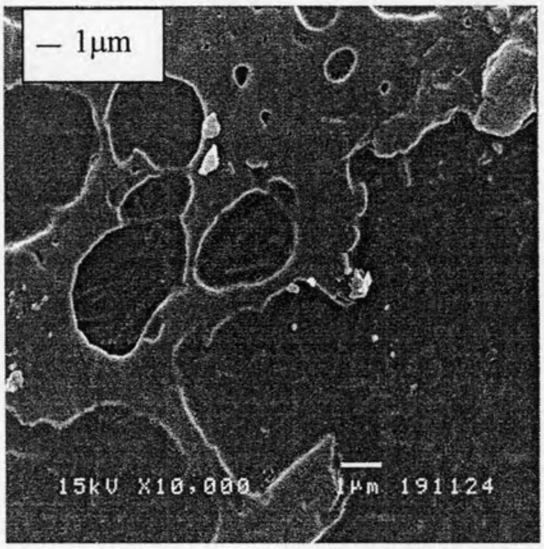

Figure 4.32 SEM image of pure PVA fibers after subjected to the solvothermal reaction in 1- octanol at 250 °C for 2 hr.

Figure 4.33 shows FT-IR spectra for the composite fibers and the final products. It can be seen that pure PVA product after solvothermal reaction still have the functional groups of PVA polymer (broad absorption bands from 2,800 to 3,000 cm^{-1} and 800 to 1,800 cm^{-1}), although part of the organic molecules of PVA are removed from the original PVA before the reaction.

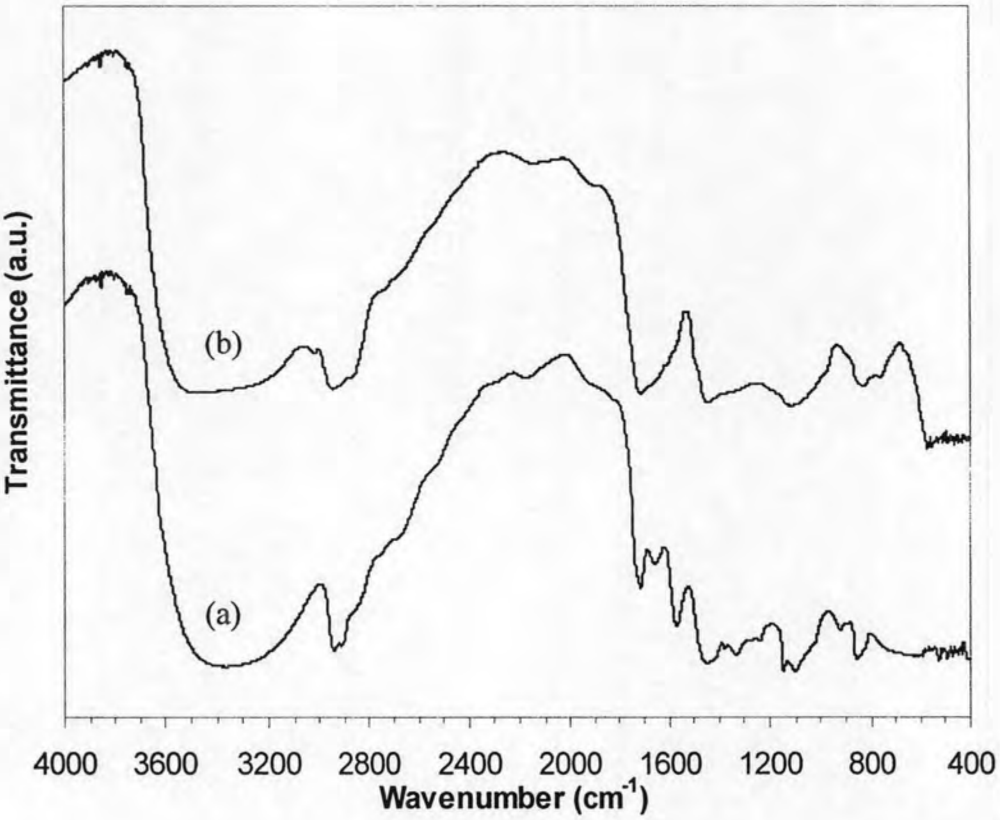

Figure 4.33 FT-IR results for pure PVA fibers (a) and PVA fibers after were added into the solvothermal system in 1- octanol at 250 °C for 2hr (b).

4.3.3.2 When PVA/zinc acetate composite fibers and excess zinc acetate powder were used as starting material

When zinc acetate powder was put into the reaction system in addition to the PVA/zinc acetate composite fibers, the obtained products could be separated into two parts, i.e. the fibers and the particles part in the same manner as previously described in section 4.2. Figure 4.34 and 4.35 show the XRD results for the fibers part and the particles part from the products synthesized at various conditions, respectively. All samples were ZnO in the hexagonal phase (wurtzite structure). A similar intensity ratio among the diffraction peaks indicates that ZnO crystals in all samples grow along the same lattice direction. From visual observation of the final products in the fibers part, it can be seen that the final product still have the elastic property of PVA.

From Figure 4.34, the peak at 2θ around 20° corresponds to (101) plane of semi-crystalline PVA in the composite fibers (Yang et al., 2000). The crystallinity of PVA is decreased when the reaction takes place at relatively high temperature, in the same manner as previously described in the results when only PVA/zinc acetate composite fibers were used as the starting material. The results also show that the intensity of XRD peaks for the particles part in the ZnO nanostructure is higher than the fibers part. It means that the particles part has higher crystallinity than the fibers part.

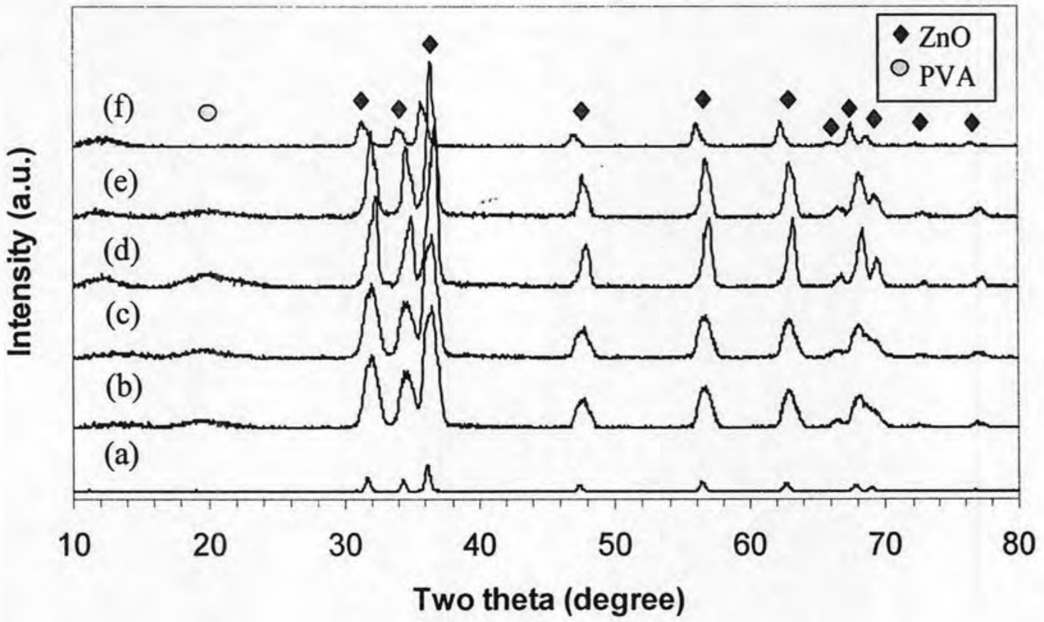

Figure 4.34 XRD results for the fibers part of the ZnO nanostructures that were synthesized from PVA/zinc acetate composite fibers and excess zinc acetate via the solvothermal reaction in 1-octanol at 170 °C for 0 hr (a), 170 °C for 2 hr (b), 200 °C for 0 hr (c), 200 °C for 2 hr (d), 250 °C for 0 hr (e) and 250 °C for 2 hr (f), using PVA-to-zinc acetate ratio of 1.5 and 10 g of excess zinc acetate powder.

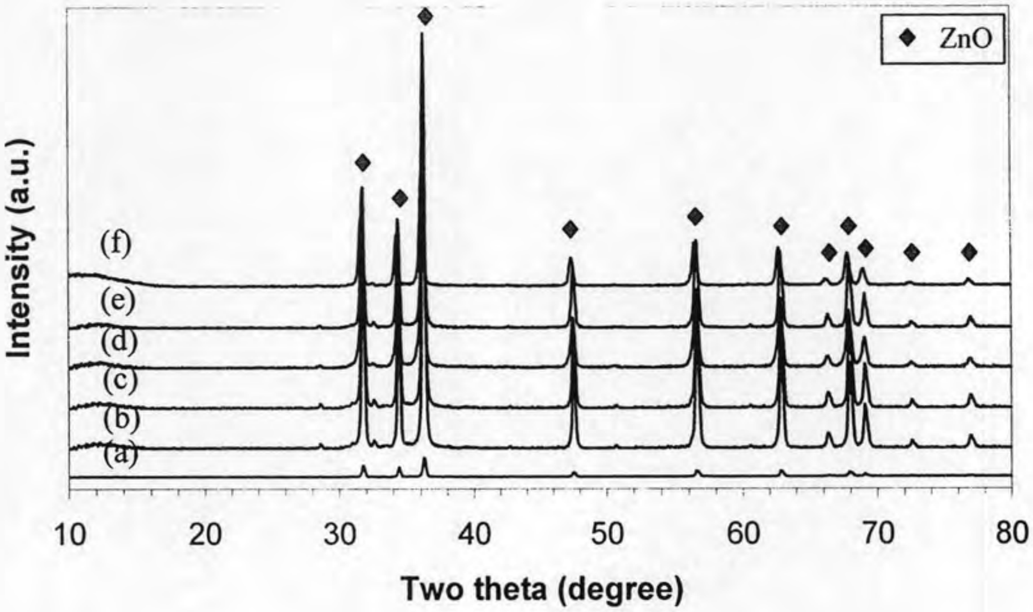

Figure 4.35 XRD results for the particles part of the ZnO nanostructures that were synthesized from PVA/zinc acetate composite fibers and excess zinc acetate via the solvothermal reaction in 1-octanol at 170 °C for 0 hr (a), 170 °C for 2 hr (b), 200 °C for 0 hr (c), 200 °C for 2 hr (d), 250 °C for 0 hr (e) and 250 °C for 2 hr (f), using PVA-to-zinc acetate ratio of 1.5 and 10 g of excess zinc acetate powder.

As discussed in Section 4.3.2, the fibers part of the obtained products are no longer observed as fibers because it is totally covered by the ZnO particles that are formed from the large quantity of the excess zinc acetate powder (i.e. 10 g).

Figure 4.36 shows SEM images of the ZnO nanostructure synthesized from PVA/zinc acetate composite fibers and 10 g of the excess zinc acetate powder, via the solvothermal reaction at 170 °C for 0 and 2 hr, respectively. It can be seen that the particles formed from the fibers part have irregular shape because the solvothermal reaction for ZnO synthesis is not completed until 200 °C (Tonto et al., 2006). The particles part of the product prepared at 170 °C for 0 hr and 2 hr composed of two types of particles, i.e. particles with irregular shape and rod-like shape. This finding may imply that the nucleation and the growth of ZnO take place continuously through out the whole reaction period. For the reaction temperature at 200 °C or higher, morphology of the obtained products shown in Figure 4.37 and 4.48 seems to be nonporous nanorod. The size distribution for diameter and length based on these SEM images are depicted in Appendix A2.

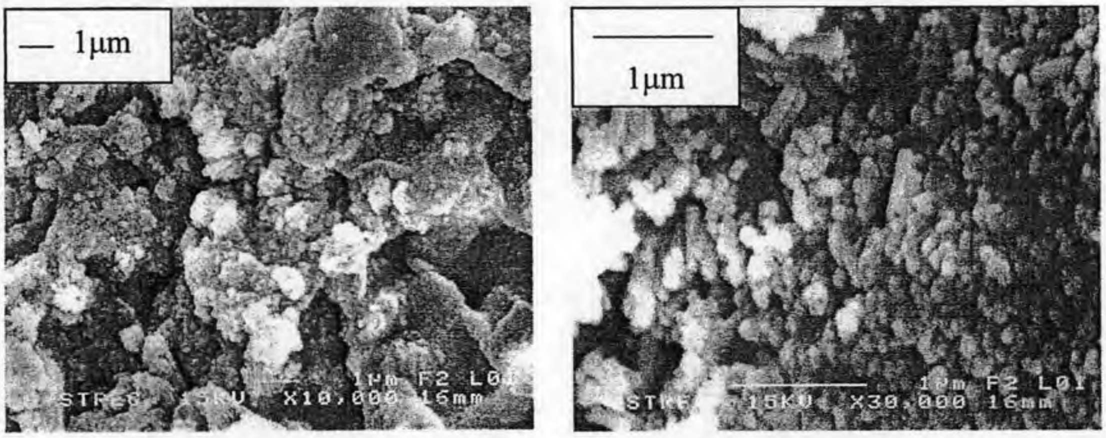

Fibers part

Particles part

(a)

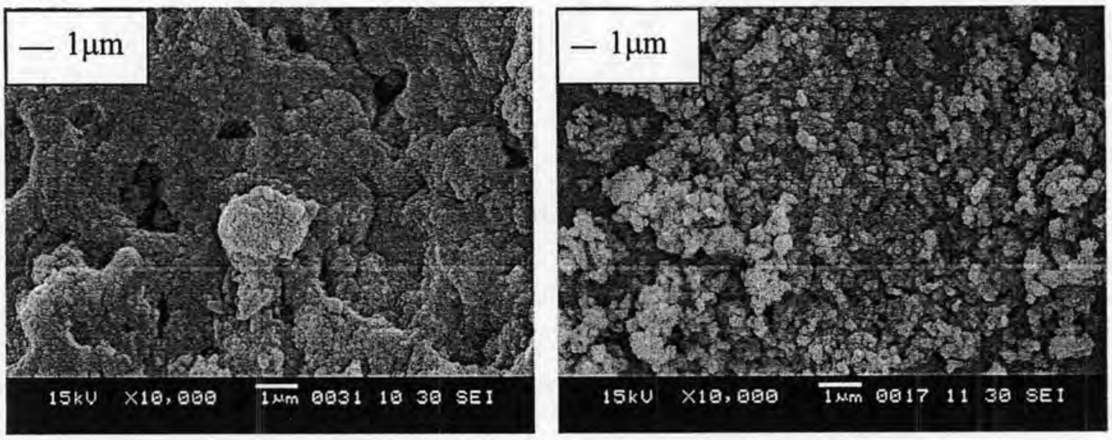

Fibers part

Particles part

(b)

Figure 4.36 SEM images of ZnO nanostructures that were synthesized from PVA/zinc acetate composite fibers with PVA-to-zinc acetate ratio of 1.5 and 10 g of excess zinc acetate powder via the solvothermal reaction in 1-octanol at 170 °C for 0 hr (a) and 2 hr (b).

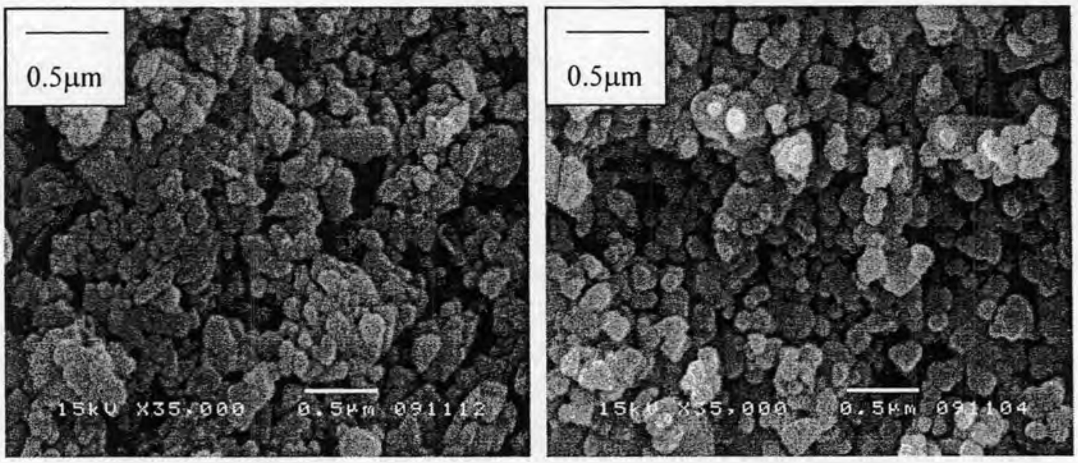

Fibers part

Particles part

(a)

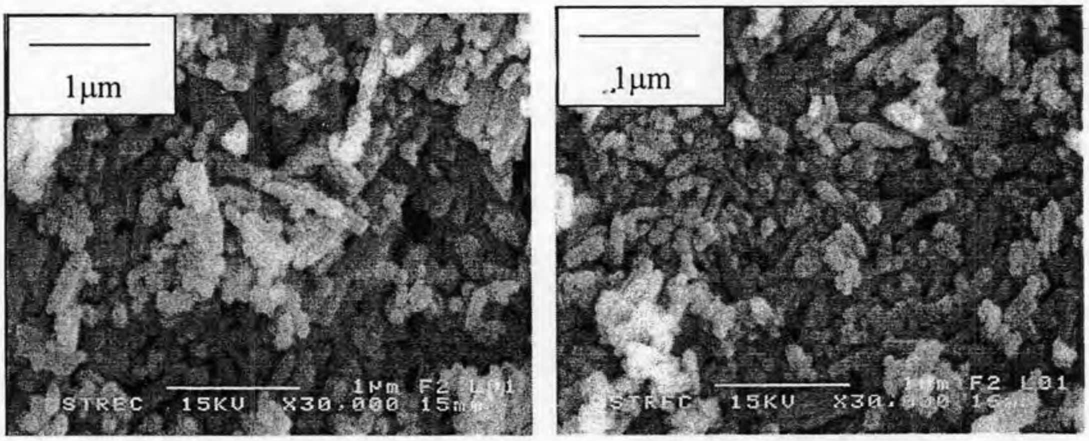

Fibers part

Particles part

(b)

Figure 4.37 SEM images of ZnO nanostructures that were synthesized from PVA/zinc acetate composite fibers with PVA-to-zinc acetate ratio of 1.5 and 10 g of excess zinc acetate powder via the solvothermal reaction in 1-octanol at 200 °C for 0 hr (a) and 2 hr (b).

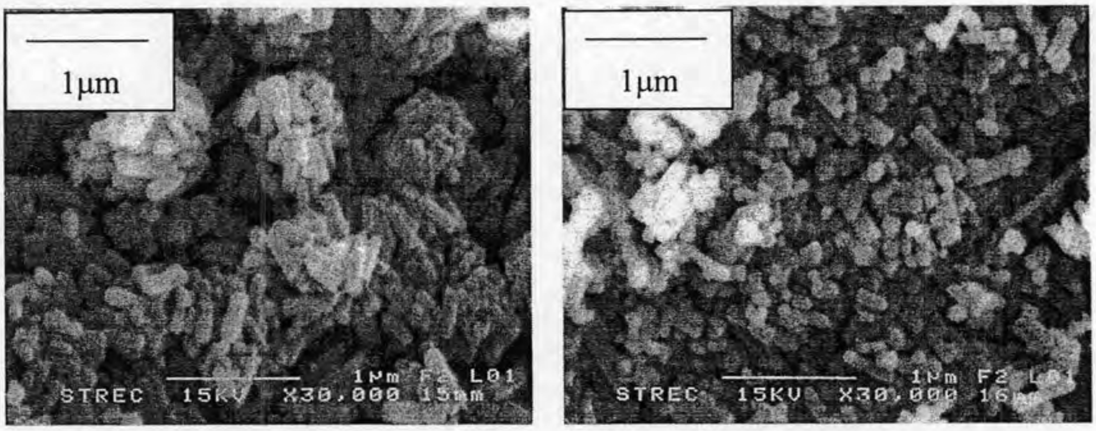

Fibers part

Particles part

(a)

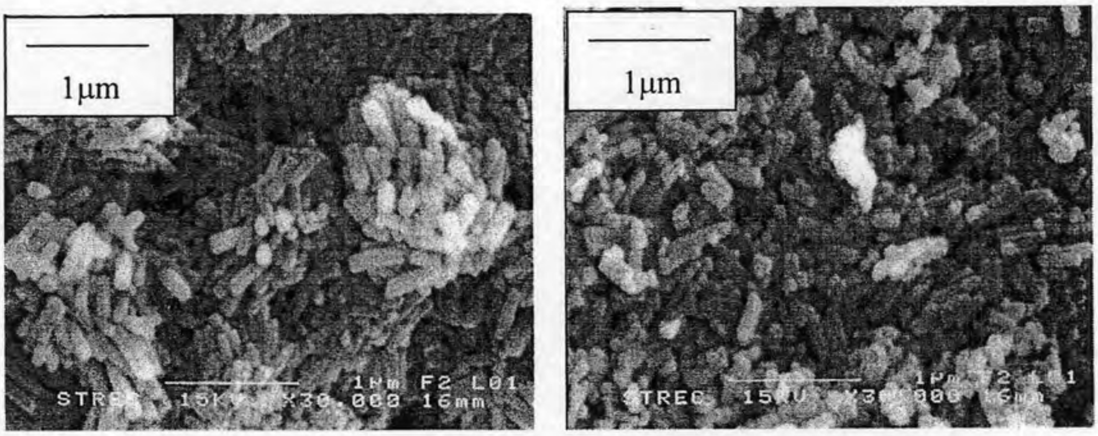

Fibers part

Particles part

(b)

Figure 4.38 SEM images of ZnO nanostructures that were synthesized from PVA/zinc acetate composite fibers with PVA-to-zinc acetate ratio of 1.5 and 10 g of excess zinc acetate powder via the solvothermal reaction in 1-octanol at 250 °C for 0 hr (a) and 2 hr (b).

Figure 3.39 and 4.40, summarize the average diameter and average length, respectively, for both fibers part and particles part of the ZnO nanostructures synthesized under various conditions. It is found that average diameter is approximately unaffected by the increase in either the reaction temperature or the reaction time. On the other hand, the average length of ZnO nanorods increases with the increase in the reaction temperature and reaction time. This observation suggests the increase in crystal growth with the energy of the system.

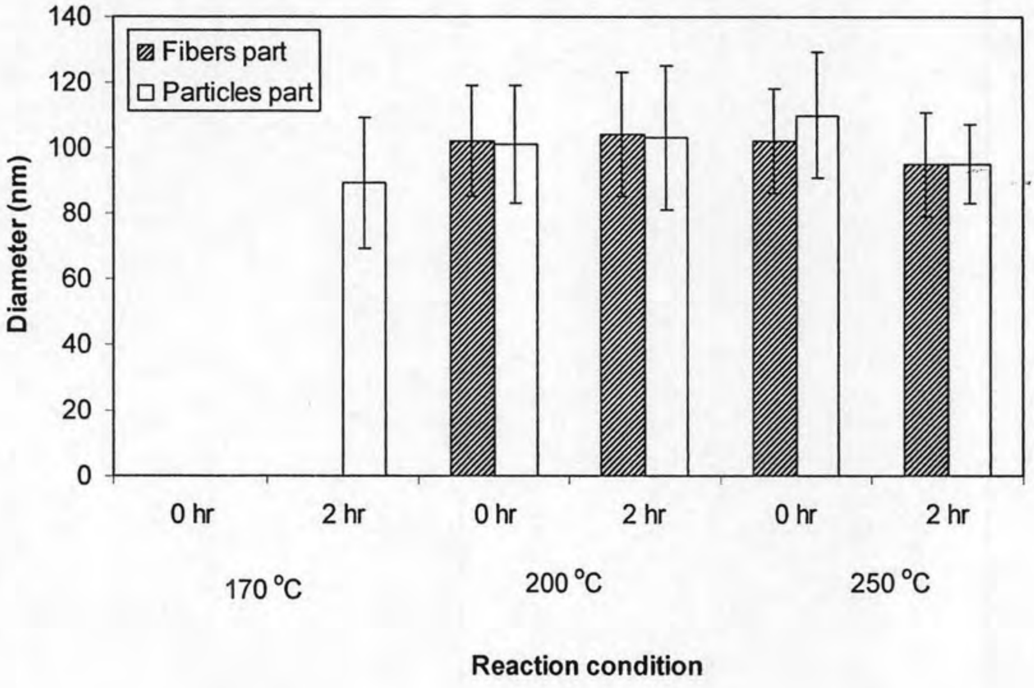

Figure 4.39 Average diameter of ZnO nanostructures that were synthesized from PVA/zinc acetate composite fibers with PVA-to-zinc acetate ratio of 1.5 and 10 g of excess zinc acetate powder via the solvothermal reaction in 1-octanol under various reaction conditions.

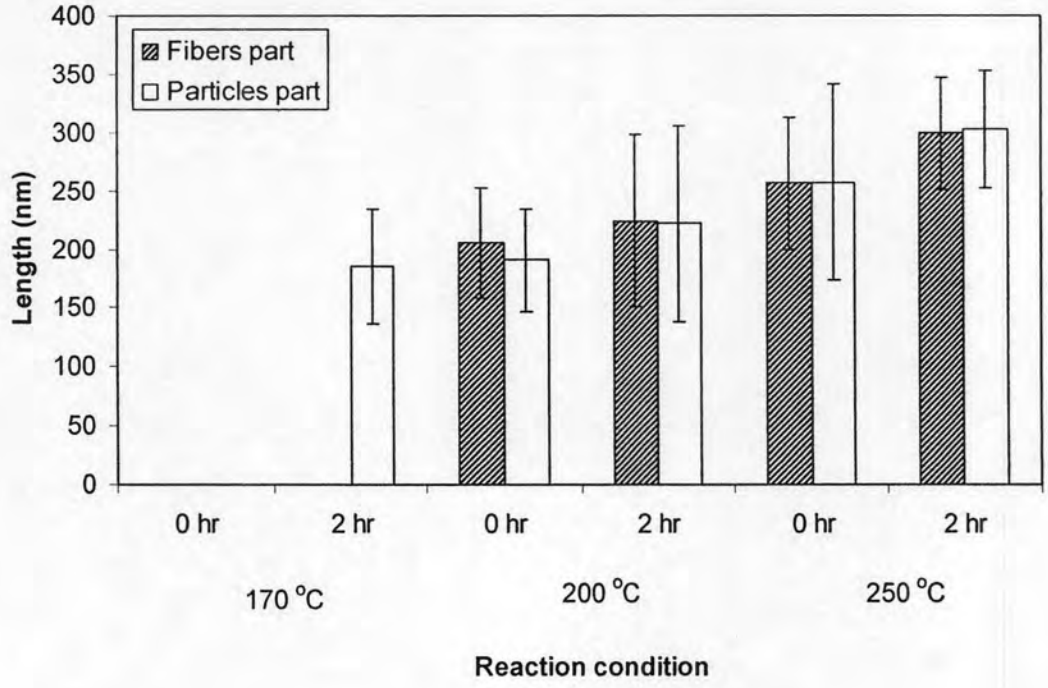

Figure 4.40 Average length of ZnO nanostructures that were synthesized from PVA/zinc acetate composite fibers with PVA-to-zinc acetate ratio of 1.5 and 10 g of excess zinc acetate powder via the solvothermal reaction in 1-octanol under various reaction conditions.

For the crystallite size shown in Figure 4.41, it can be observed that the crystallite sizes of all obtained products are smaller than the size of the obtained products observed from SEM images. This observation suggests that all of the obtained products are polycrystals. The trend for the change of the crystallite size from the change in the reaction conditions is similar to that discussed in Section 4.3.3.1. Moreover, the crystallite size of the fibers part is smaller than that of the particles part. This observation suggests that the polymer, i.e. PVA, inhibits the growth of ZnO nanocrystals within the fiber.

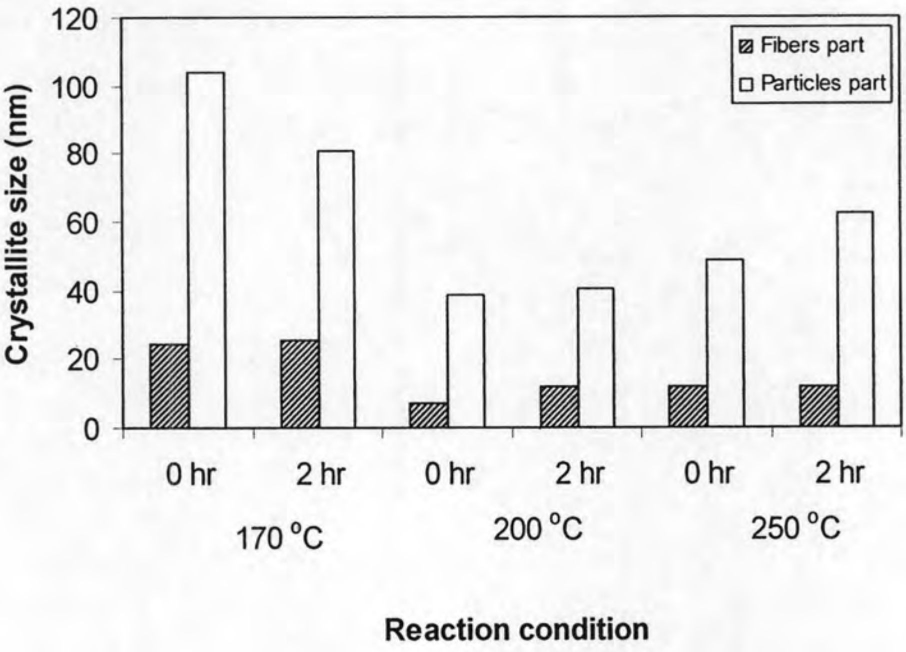

Figure 4.41 Crystallite size of ZnO nanostructure that were synthesized from PVA/zinc acetate composite fibers with PVA-to-zinc acetate ratio of 1.5 and 10 g of excess zinc acetate powder via the solvothermal reaction in 1-octanol under various reaction conditions.

Figure 4.42 shows the FT-IR spectra of the fibers part of the products synthesized under various conditions of the reaction temperatures and reaction times. All final products still have the functional groups of PVA (broad absorption bands from 2,800 to 3,000 cm^{-1} and 800 to 1800 cm^{-1}) (Hui et al., 2006). When both the reaction temperature and the reaction time are increased, the signals from these functional groups are decreased, indicating that some parts of the organic moiety of PVA are removed from the composite fibers.

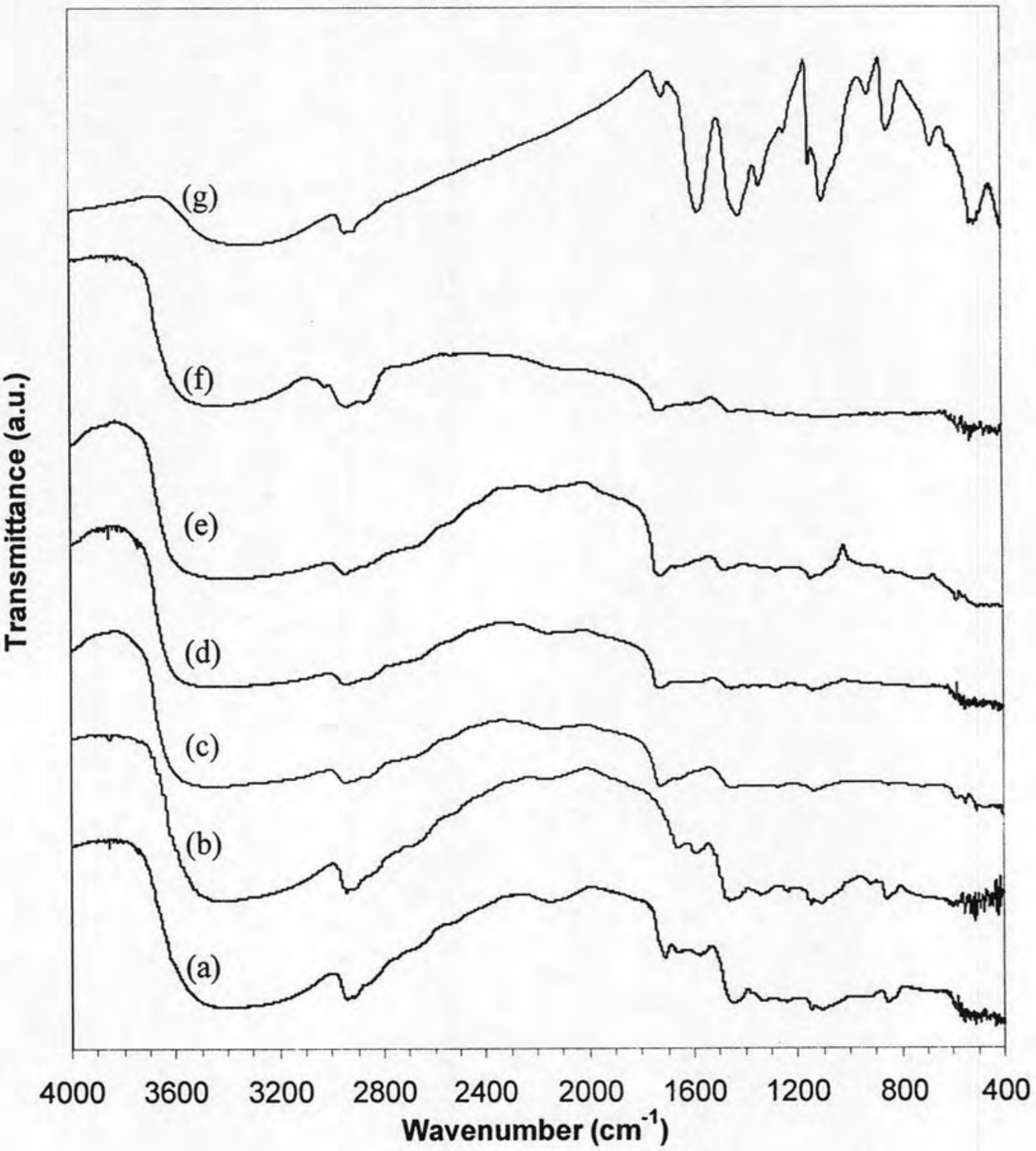

Figure 4.42 FT-IR spectra for the fibers part of the ZnO nanostructure that were synthesized from PVA/zinc acetate composite fibers and excess zinc acetate via the solvothermal reaction in 1-octanol at 170 °C for 0 hr (a), 170 °C for 2 hr (b), 200 °C for 0 hr (c), 200 °C for 2 hr (d), 250 °C for 0 hr (e) and 250 °C for 2 hr (f), comparing with that of PVA/zinc acetate composite fibers (g), using PVA-to-zinc acetate ratio of 1.5 and the excess zinc acetate powder of 10 g.

Figure 4.43 shows the FT-IR spectra of the particles part of the obtained products. Two broad peaks at about 1,600 and 1,451 cm^{-1} are clearly seen. When the reaction temperature and the reaction time are increased, the intensity of these two bands is decreased and almost diminished at the reaction temperature of 250 ^{o}C. This observation suggests that zinc acetate is not completely converted into ZnO at low reaction temperature.

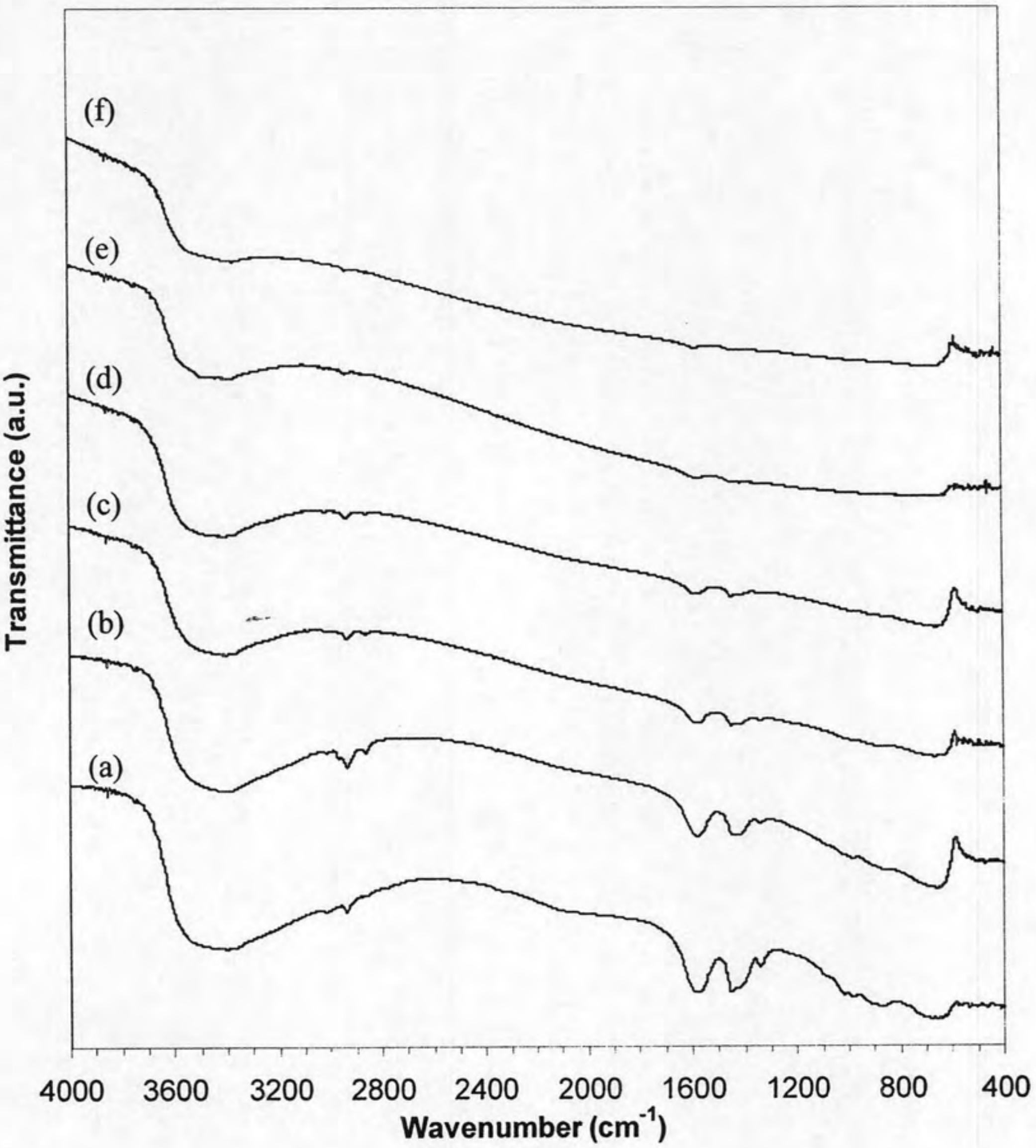

Figure 4.43 FT-IR spectra for the particles part of the ZnO nanostructure that were synthesized from PVA/zinc acetate composite fibers and excess zinc acetate via the solvothermal reaction in 1-octanol at 170 °C for 0 hr (a), 170 °C for 2 hr (b), 200 °C for 0 hr (c), 200 °C for 2 hr (d), 250 °C for 0 hr (e) and 250 °C for 2 hr (f), comparing with that of PVA/zinc acetate composite fibers (g), using PVA-to-zinc acetate ratio of 1.5 and the excess zinc acetate powder of 10 g.

4.4 Comparison between Calcined Products and Solvothermal Products

The morphology of the calcined fibers was discussed in Section 4.1. These products were obtained by high temperature calcination of the PVA/zinc acetate composite fibers. It was generally observed that the calcination temperature has a great influence on both the crystalline phase and the surface morphology of the fibers (Chronakis 2005). The PVA inside the composite fibers was completely removed and zinc acetate was decomposed under high temperature. The removal of PVA also reduces elasticity of composite fibers. According to literature review, tensile test of ceramic nanofibers has been done using a nano tensile tester (Zussman et.al, 2003). These tested fibers exhibited the characteristic low strength and low modulus but high extensibility at room temperature. The mechanical properties were also found to be dependent on fibers diameter. Fibers with a smaller diameter had a higher strength but lower ductility (Chronakis 2005).

The morphology of the solvothermal products was discussed in Section 4.2. Moreover, Tonto et al. (2006) investigated the reaction mechanism of the solvothermal process when 1-octanol was used as solvent. The solvent recovered after the reaction was collected and analyzed by gas chromatography. Ester and water were detected in the remaining solvents. Therefore, it was proposed that the interaction between zinc acetate and alcohol under the solvothermal conditions resulted in esterification reaction, which proceeded to form ZnO, ester and water, according to the following reaction:

$$Zn(CH_3COO)_2 + 2R\text{-}OH \leftrightarrow ZnO + 2CH_3\text{-}CO\text{-}R + H_2O$$

Once the ZnO seeds were formed, further reaction resulted in crystal growth of ZnO nanoparticles. The size and shape of the particles were controlled by the reaction conditions (Tonto et al., 2006).

In this work, ZnO nanostructures that were synthesized from PVA/zinc acetate composite fibers via the solvothermal reaction in 1-octanol at various reaction temperatures and reaction times were calcined at the same condition as the directly cacined products, i.e. 600 °C. Figure 4.44 shows the XRD results for the final products. All samples were ZnO in the hexagonal phase (wurtzite structure) without contamination from other crystalline phase. A similar intensity ratio of the diffraction peaks indicates that ZnO crystals grow along the same lattice direction. Moreover, the intensity from the calcined products seems to be higher than the products before calcination (comparing with XRD results in Figure 4.24). This observation suggests that the crystallinity of the products is increased by high temperature.

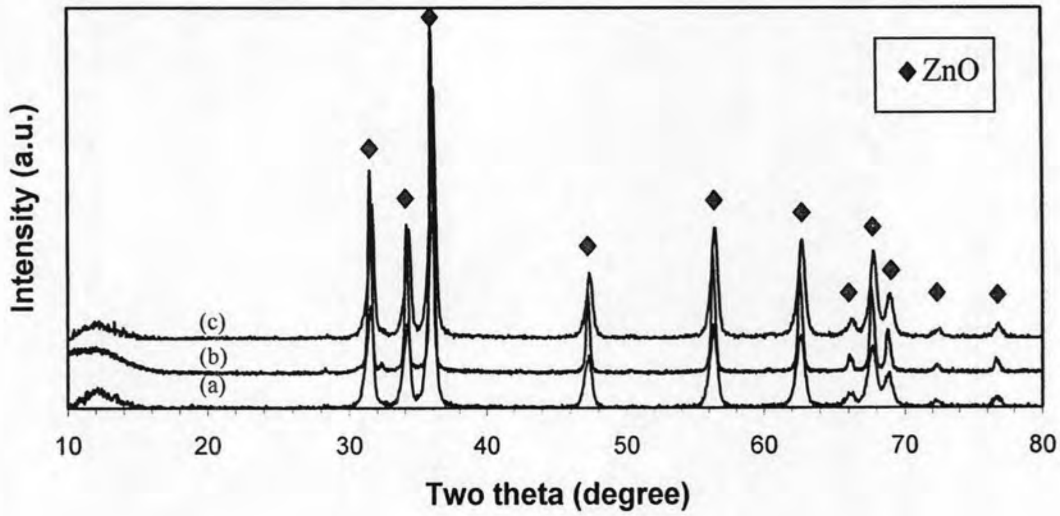

Figure 4.44 XRD results for the ZnO nanostructures that were synthesized from PVA/zinc acetate composite fibers with PVA-to-zinc acetate ratio of 1.5 via the solvothermal reaction in 1-octanol, at 170 °C (a), 200 °C (b) and 250 °C (c) for 2 hr and subsequently calcined at 600 °C for 2 hr.

Figure 4.45 shows SEM images of the final products after calcinations at 600 °C. It is found that the fiber form of the final products could no longer be seen because the PVA within the fiber was completely removed. They are difference from the products synthesized via the calcination of PVA/zinc acetate composite fibers (i.e., the direct calcined products) because ZnO particles in the direct calcined products are resulted from thermal decomposition of zinc acetate but the ZnO particles in the solvothermal products are resulted from the reaction between zinc acetate and 1-octanol. The subsequent calcination mainly removes left-over PVA in the products. Figure 4.46 shows the size distribution of the final products from the solvothermal and subsequently calcinations processes. It can be seen that the average diameter of ZnO particles within the final products are nearly the same. This observation suggests that the effect from subsequent high-temperature calcination dominates the difference in morphology of the as-obtained products from the solvothermal process. At high temperature all organic molecules within the fibers were completely removed and zinc acetate was completely converted to ZnO.

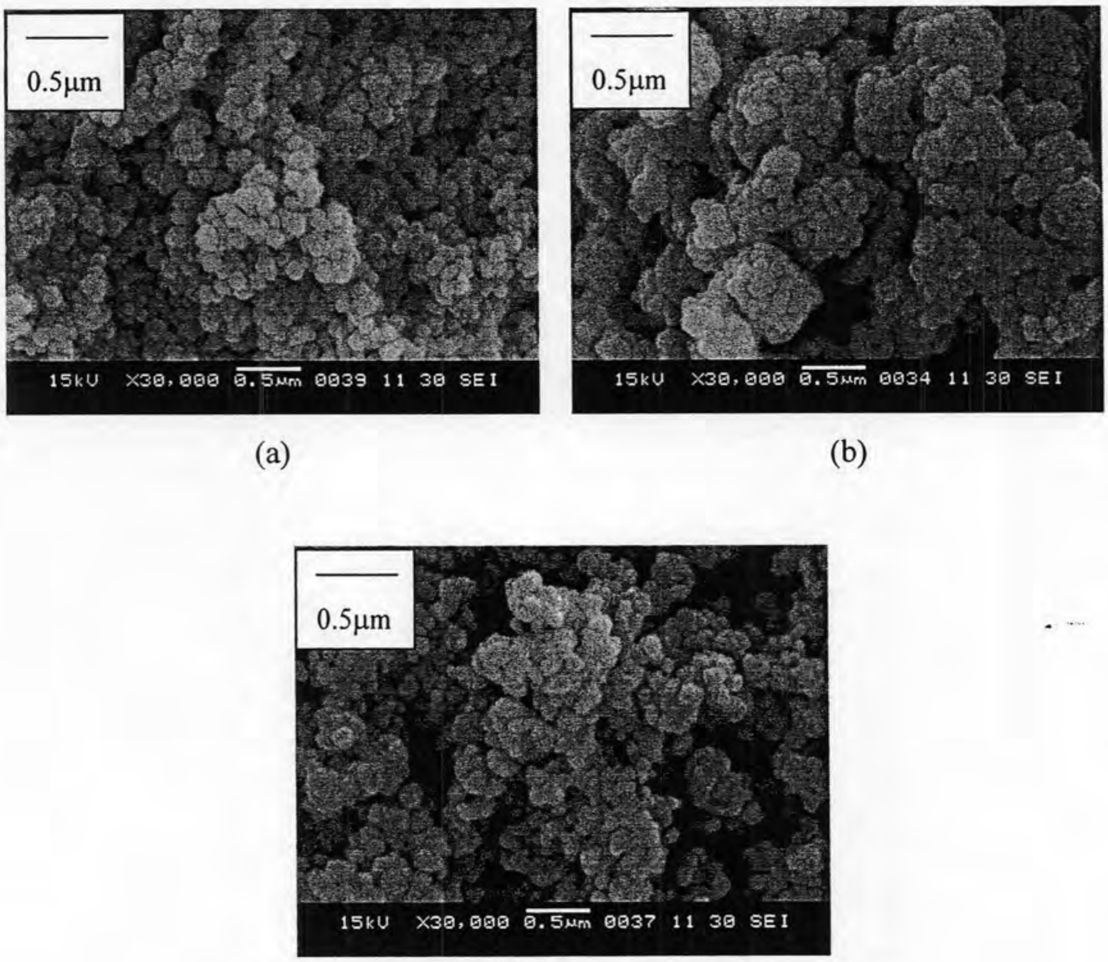

(a) (b)

(c)

Figure 4.45 SEM images for the ZnO nanostructures that were synthesized from PVA/zinc acetate composite fibers with PVA-to-zinc acetate ratio of 1.5 via the solvothermal reaction in 1-octanol, at 170 °C (a), 200 °C (b) and 250 °C (c) for 2 hr and subsequently calcined at 600 °C for 2 hr.

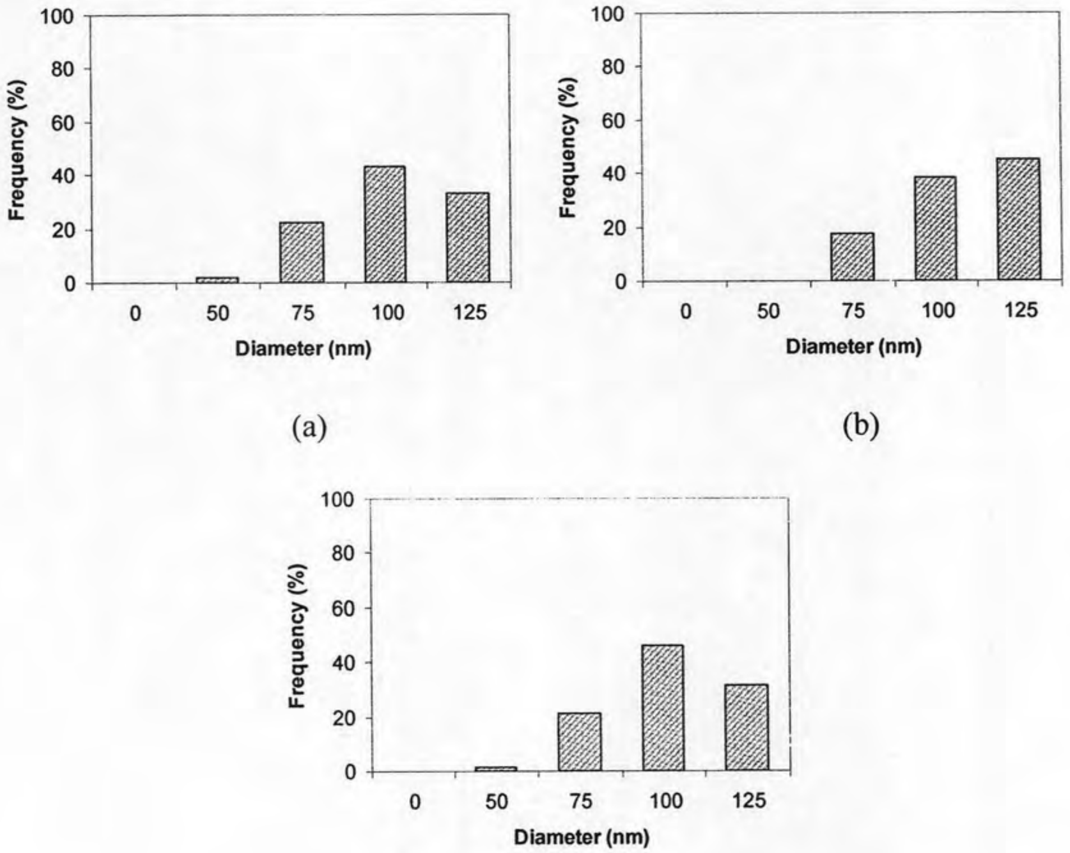

(a)

(b)

(c)

Figure 4.46 Size distributions for the ZnO nanostructures that were synthesized from PVA/zinc acetate composite fibers with PVA-to-zinc acetate ratio of 1.5 via the solvothermal reaction in 1-octanol, at 170 °C (a), 200 °C (b) and 250 °C (c) for 2 hr and subsequently calcined at 600 °C for 2 hr.

Figure 4.47 shows FT-IR results of the final solvothermal products after calcination. The results indicate that all organic molecules are completely removed from the solvothermal products after calcination at 600 °C for 2 hr (comparing with results in Figure 4.30), since all the absorption bands associated with organic species at wavenumber in the range of 800 – 1800 cm^{-1} are disappeared (Siddheswaran et al., 2006).

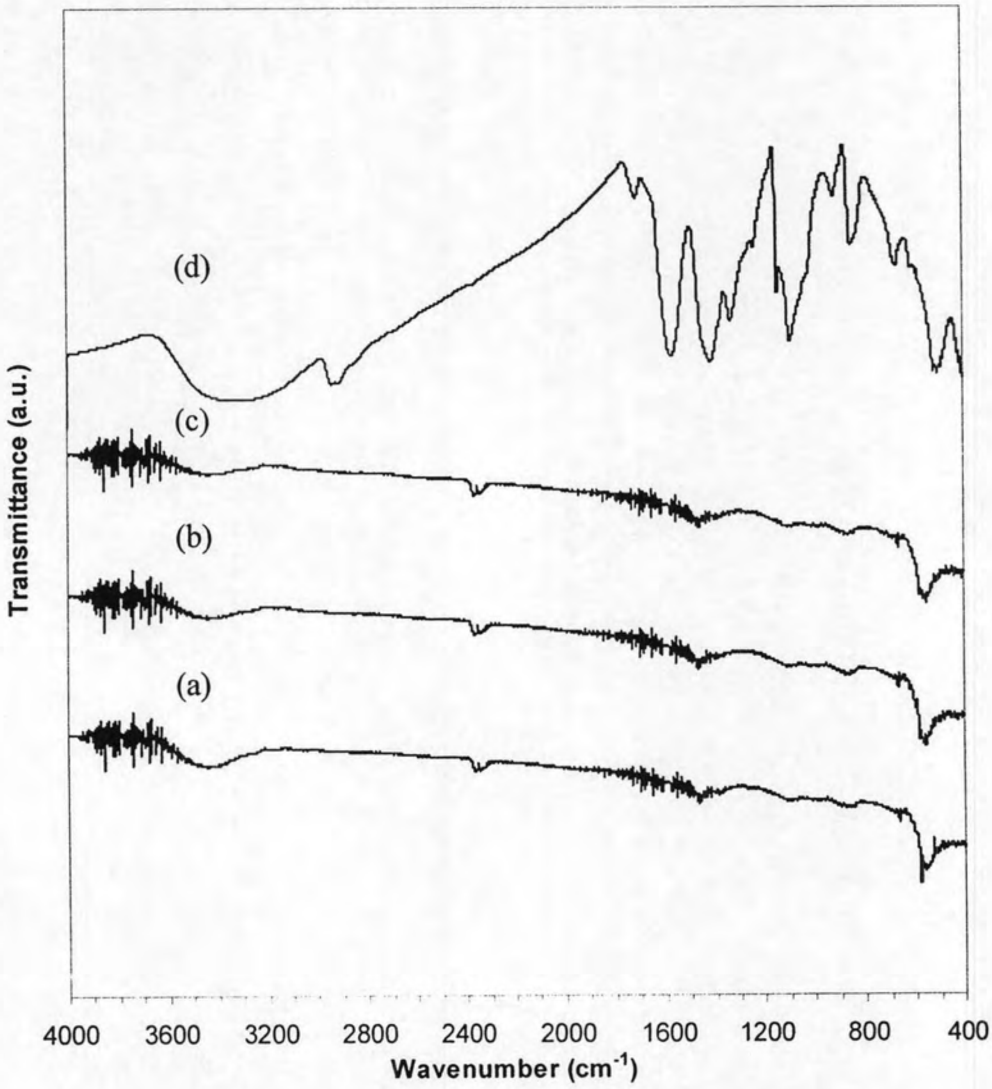

Figure 4.47 FT-IR results for calcined products that were synthesized from ZnO nanostructures that were synthesis from PVA/zinc acetate composite fibers via the solvothermal reaction in 1-octanol, calcined at 600 °C for 2hr: the conditions of solvothermal, using PVA-to-zinc acetate ratio of 1.5 at 170 °C for 2 hr (a), 200 °C for 0 hr (b) and 250 °C for 2 hr (c), comparing with that of PVA/zinc acetate composite fibers (d).

For the ZnO nanostructures that were synthesized from the direct calcination of the PVA/zinc acetate composite fibers at 250 °C for 2 hr (the same temperature and time as those employ in the solvothermal process), Figure 4.48 shows that the product is ZnO in the hexagonal phase (wurtzite structure) without contamination from other crystalline phase. Nevertheless, the intensity ratio among peaks in Figure 4.48 is different from those observed in the previous Section. Moreover, some peaks are merged together. This observation suggests that ZnO crystals in this case grow along different lattice direction than the ones observed earlier. It might be the result from the calcination temperature that is so low that zinc acetate may not completely decomposed under atmospheric pressure.

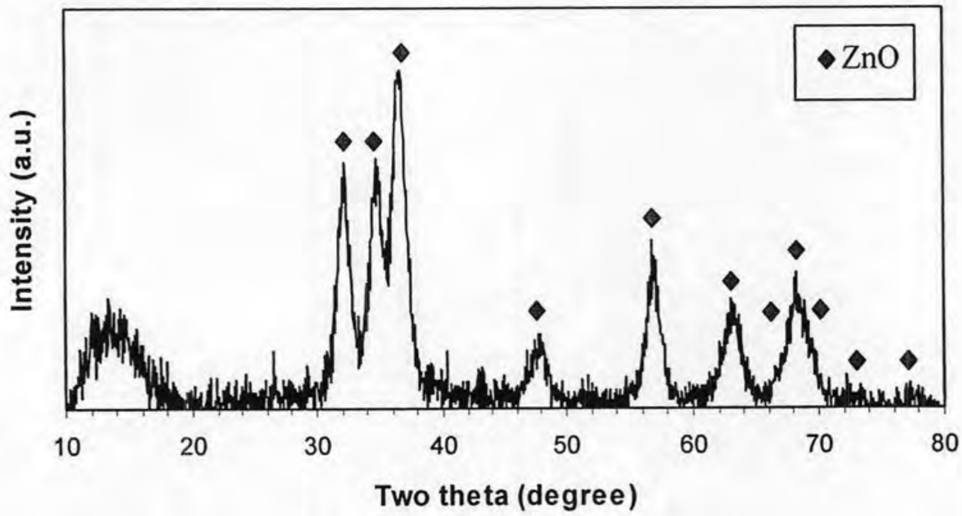

Figure 4.48 XRD result of PVA/zinc acetate fibers directly calcined at 250 °C for 2 hr.

Figure 4.49 shows the SEM images of the PVA/zinc acetate composite fibers that were calcined at 250 °C for 2 hr. It can be observed that the calcined fibers have relatively smooth surface and narrow size distribution around 150 nm as shown in Figure 4.50. However, the ZnO fibers obtained exhibit significant shrinkage as well as a reduction in fiber diameter (compared with the pre calcined fibers in Figure 4.1(c)) due to the decomposition of PVA and the removal of organic content. From the TG curve in Figure 4.11(a), PVA should be completely removed at 500 °C. At this condition PVA is still retain in the fibers but all the functional grops of PVA are completely removed from the fibers. It is confirmed by FT-IR results are shown in Figure 4.51 and TG curve in Figure 4.52. This observation suggests that, although low calcination temperature is used to convert PVA/zinc acetate composite fibers directly into ZnO fibers while retaining PVA in the fibers, elasticity property of PVA is lost.

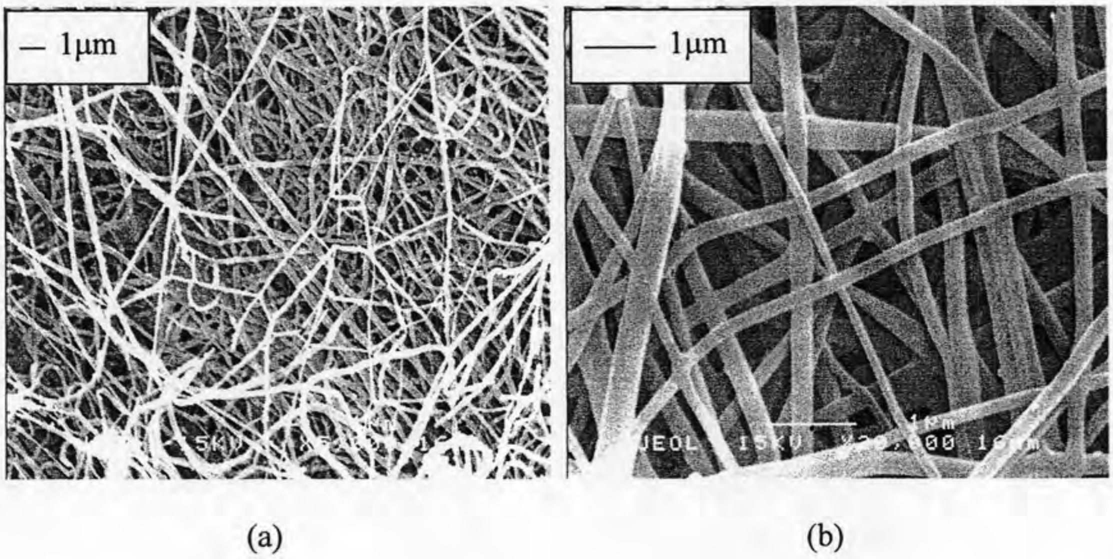

Figure 4.49 SEM images of PVA/zinc acetate fibers directly calcined at 250 °C for 2 hr: (a) low magnification (b) high magnification.

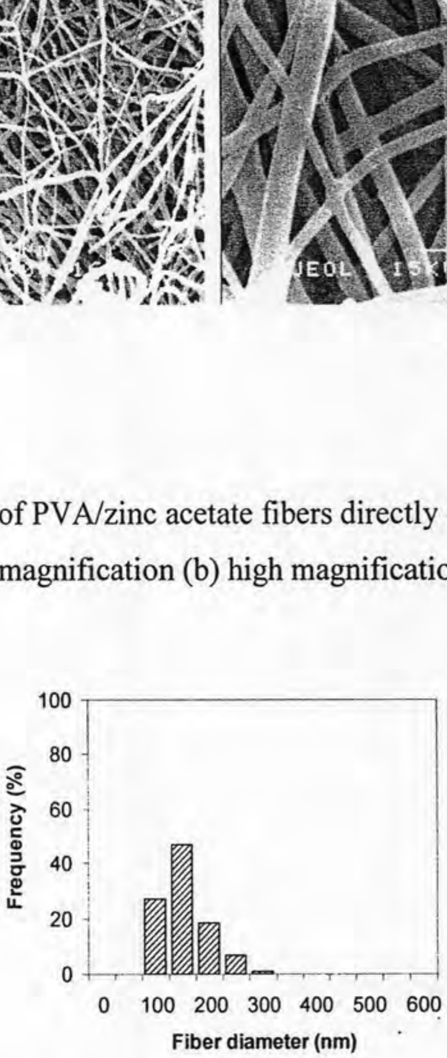

Figure 4.50 Size distribution of PVA/zinc acetate fibers directly calcined at 250 °C for 2 hr.

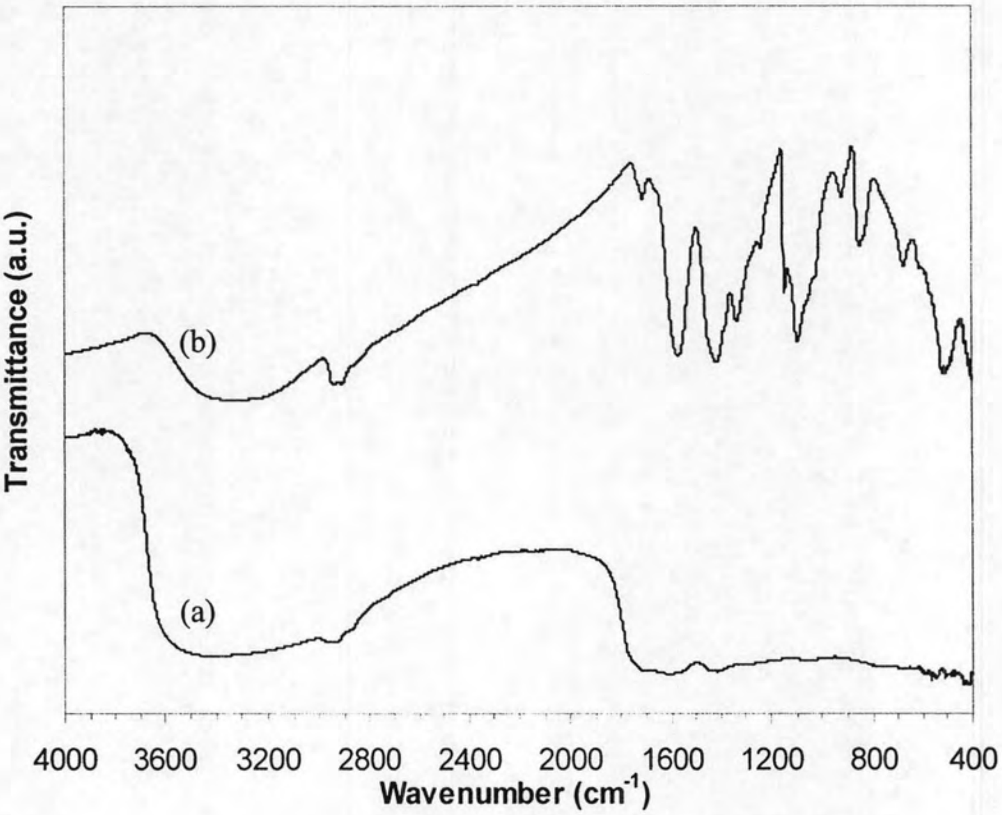

Figure 4.51 FT-IR results of PVA/zinc acetate fibers directly calcined at 250 °C for 2 hr (a) comparing with PVA/zinc acetate composite fibers (b).

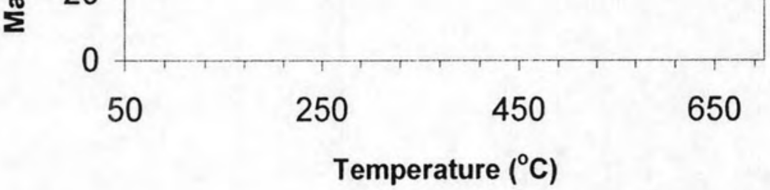

Figure 4.52 Thermogravimetric curve of PVA/zinc acetate fibers directly calcined at 250 °C for 2 hr.